전 용 필 교수지도

석사학위 청구논문

Modification of the expression profiles of *Prnp* and marker genes in early stage embryo by DNMT1 modulators

2024

성신여자대학교 대학원

생물학과

조 정 빈

Modification of the expression profiles of *Prnp* and marker genes in early stage embryo by DNMT1 modulators

Adviser: Yong-Pil Cheon, Ph.D.

Submitted in partical fulfillment
of the requirements for the degree of master.

May, 2024

Department of Biology

The Graduate School of Sungshin University

Jeong Bin Jo

This is certify that we have examined the

Master's Thesis of

Jeong Bin Jo

Submitted to Department of Biology

Approved as to style and content

Thesis Advisor .....

Committee Chairman .....

Committee Member .....

Committee Member .....

The Graduate School of Sungshin University

ABSTRACT

Modification of the expression profiles of *Prnp* and marker genes in early stage embryo by DNMT1 modulators

Jeong Bin Jo
Department of Biology
Graduate School
Sungshin University

The products of *Prnp* gene are the functional molecule in development, physiology and disease. One of the possible reasons of prion disease is the amount of cellular prion protein (PrP^C) in a tissue, and controlling the expression levels of PrP^C is suspected as a way of protection the prion. In addition, PrP^C can affect stem cell proliferation, metastasis, drug resistant, and cancer stem cell phenotypes through several signaling pathways as a platform. Therefore, it is important to know the expression profiles during development. On the other hand, DNA methylation is a major epigenetic mechanism and plays critical roles in the silencing of retrotransposons, genomic imprinting, and cell differentiation. Even though the mechanisms of epigenetic modification are not fully unmasked during cleavage, the epigenetic modification is well studied. In this study, the

expression of the *Prnp* was examined in the cleavage stage and the changes of developmental genes by DNMT1 modifying molecules, S-adenosyl-homocysteine (SAH), N-phthalyl-L-tryptophan (RG108), and maybridge (Myb1) in WT and bankvole Prnp KI mouse. The developmental rates were high in DNMT1 modulator treated groups with exception. In wild type mice, the development to the hatched stage was similar between group excepted SAH group. Developmental rate to hatched stage were significantly high in Myb1 group. In SAH group, the developmental rate was significantly lower after blastocyst stage compared to the other groups. On the other hand, in bank vole Knock-in mice, the developmental rates were significantly low after 4-cell stage in SAH group. The expression of the potency and lineage related genes such as *MuERV-L, Cdx2, Sox2, Cx32, Dsc2*, *Yap, Cdh1, Pou5f1, Nanog* were also modified with the inhibitor specific patterns. In WT, the SAH-treated particularly aberrant expression in these genes, as did the developmental rate decrease. On the one hand, *Cdx2* expression was increased in 8-cell stage embryos treated with Myb1, and *Pou5f1* gene level was also significantly increased compared to other groups after morula stage. Similarly, KI mice showed decreased expression of the above genes in SAH-treated embryos, and Myb1 treatment significantly increased *Pou5f1* gene levels at the blastoderm stage of hatching progression. The expression of imprinting genes and DNMT enzyme genes were also analyzed and did not show significant changes in WT and KI mice. To investigate whether DNMT1 inhibitors affect *PRNP* expression, it was also identified that the expression profiles of *Prnp* and PrP^c in mouse early embryo. In the wild type, mRNA expression did not show any significant change, but PrP^c protein was significantly increased at the morula stage compared to the control. In KI mice, there was a significant increase in both mRNA and protein in RG108-treated

morula stage embryos. To investigate whether the above DNMT1 inhibitors regulate expression by modulating the methylation of the CpG region of the *Prnp* gene, we performed bisulfite sequencing and found that *Prnp* expression is not regulated through this region. We then examined the effects of DNMT1 inhibitor treatment on embryo development and growth by DNMT inhibitor treated embryo transfer into surrogate mothers. Myb1 treatment significantly increased the probability of live birth after embryo transfer compared to the control group and significantly decreased in SAH-treated embryos. Organ weights of 5-week-old pups born after embryo transfer were no differences in all groups. RNA-seq results showed the high expression of carbohydrate metabolic genes in Myb1 treated embryos, immune related genes in SAH, and cell proliferation related genes in RG108. Put together, it is suggested that the gene expression is modified with the DNMT1 inhibitor specific manner and Myb1 is a useful DNMT1 inhibitor for the early stage embryo development along with the regulation of *Prnp* expression.

CONTENTS

List of Tables

List of Figures

INTRODUCTION

Prions are proteinaceous infectious particles that cause contagious or genetic neurodegenerative diseases. Creutzfeldt-Jakob disease (CDJ) and Gerstmann-Straussler-Scheinker disease in humans, and scrapie and bovine spongiform encephalopathy (BSE) in animals (Chen et al., 1994). Prions are made from normal cellular prion protein (PrP^{c}) found throughout the body of healthy people and animals. The prion protein is a conserved glycoprotein tethered to cell membranes by a glycosylphosphatidylinositol (GPI) anchor (Prusiner, 1998). However, the prion protein found in infectious substances has a different structure from these proteins and is not easily degraded by protease (Suzette, 2003). Infectious prion particles consist largely, if not all, of an aberrant isoform of a prion protein encoded by a chromosomal gene. PrP^{c} misfolding is facilitated by the conformational change of α-helix-rich cellular PrP to β-sheet-rich scrapie PrP (PrP^{SC}) followed by the formation of insoluble aggregates of misfolded PrP^{SC} (Caughey et al., 2009). PrP^{C} could be detected not only in neuronal cells but also in specific non-neuronal cells in the regional and temporal gene expression of prenatal PrP (Manson et al., 1992). And recent studies have shown that it affects cell proliferation, metastasis, drug resistance, and cancel stem cell phenotypes through several signaling pathways (Go et al., 2020). In particular, studies related of *Prnp*, differentiation, potency and stemness are being conducted in stem cell-related studies. *Prnp* was found to participate in the transcription of a pluripotency marker such as Nanog during embryonic stem cell differentiation (Miranda et al., 2011). In cancer stem cell, PrP^{c} directly regulates stem cell marker such as Oct4 (Lee et al., 2018). These results suggest that *Prnp* genes are involved in the regulation of expression of genes involved in preimplantation embryo development.

Methylation and demethylation of DNA are a crucial epigenetic mechanism and plays critical roles in transcriptional repression or activation, X-chromosome inactivation, cell differentiation, and tumorigenesis (Uysal et al. 2015). DNA methylation is especially catalyzed by several types of DNA methyltransferase (DNMT) enzymes. The DNMT1 protein primarily functions in maintenance methylation by adding methyl groups to the hemi-methylated DNA strands during DNA replication (Bestor, 2000). Recent studies have shown that DNMT1 regulates the timing and genomic targets of *de novo* methylation by DNMT3b in mouse embryonic stem cells (Ito et al., 2022), and has *de novo* activity on transposable elements (Haggerty et al., 2021). Both DNMT3a and DNMT3b essentially implicate in the *de novo* methylation process, commonly being appeared in the unmethylated DNA strands at the CpG islands (TurekPlewa and Jagodzinski 2005). DNMT3l induces the recruitment or activation of DNMT3a and 3b (Klose et al., 2006). DNMT2 is involved in tRNA methylation activity (Jeltsch et al., 2017). During oogenesis and preimplantation embryo development, DNA methylation plays critical roles in strictly regulating stimulation or repression of the development related genes and in timely establishing maternal and paternal imprints (Bartolomei and Ferguson-Smith 2011). Two isoforms of Dnmt1 have been identified in the mouse (Carlson et al., 1992) and homologues have been identified in humans (Hayward et al., 2003): an oocyte-specific isoform (DNMT1o) found only in oocytes and cleavage stage preimplantation embryos and a somatic form (DNMT1s). DNMT1s express during oocyte and early embryo stage in nucleus. DNMT1o is present in the cytoplasm and undergoes a transition to the nucleus at the 8-cell stage (Fig. 1). DNMT3a is cytoplasmic in oocytes and then expressed in the nucleus in early embryos. DNMT3b is expressed in the nucleus from the 4-cell stage embryo (Petrussa et al., 2014).

The DNA methyltransferase inhibitor (DNMTi) is used as potential anticancer

drugs in cancer therapy such as colon, ovarian, and lung cancer and tumor immunotherapy (Lyko et al., 2005). In addition, DNMTi is also widely used in somatic cell nuclear transfer (SCNT) embryos to overcome epigenetic inhibition (Dean et al., 2001) and gene expression (Humpherys et al., 2003). In SCNT embryos, reprogramming of the nucleus of the oocyte or embryo by substituting nuclei of somatic cell is required (Wei eat al., 2011). DNMT1 inhibitors are often used to overcome abnormal epigenetic modifications caused by DNMT1s of somatic cell origin. Previous studies have shown that X-chromosome inactivation and in vitro development were improved when SAH, a competitive inhibitor for DNMT1, was treated during mouse SCNT at a concentration of 1 mM (Jeon et al., 2008). And RG108, a non-nucleoside inhibitor that inhibits enzyme activity by binding to the DNMT active site, improved epigenetic reprogramming in porcine (Zhai et al., 2018) and buffalo (Sun et al., 2016) SCNT embryo treated with 20μM.

Besides, The *Prnp* expression or localization in mouse early embryo has not been revealed. Many studies have been conducted on methylation profiling during oogenesis and embryo development, little is known about the methylation pattern of *Prnp* gene during early stage embryo. In here, the possible role of DNMT1 inhibitor (Myb1, SAH, RG108) was examined. The developmental rate and methylation pattern at 2-cell, 4-cell, 8-cell, morula, blastocyst stage embryos in vitro culture were analyzed. Collectively, the effect of myb1 on early embryo development was evaluated. In addition, the effect of CpG methylation change on the *Prnp* promoter region in mouse embryos was investigated, and *Prnp* gene expression profiling was performed accordingly. Our results provide how *Prnp* is altered by DNMT1 inhibitors treated during early embryonic development.

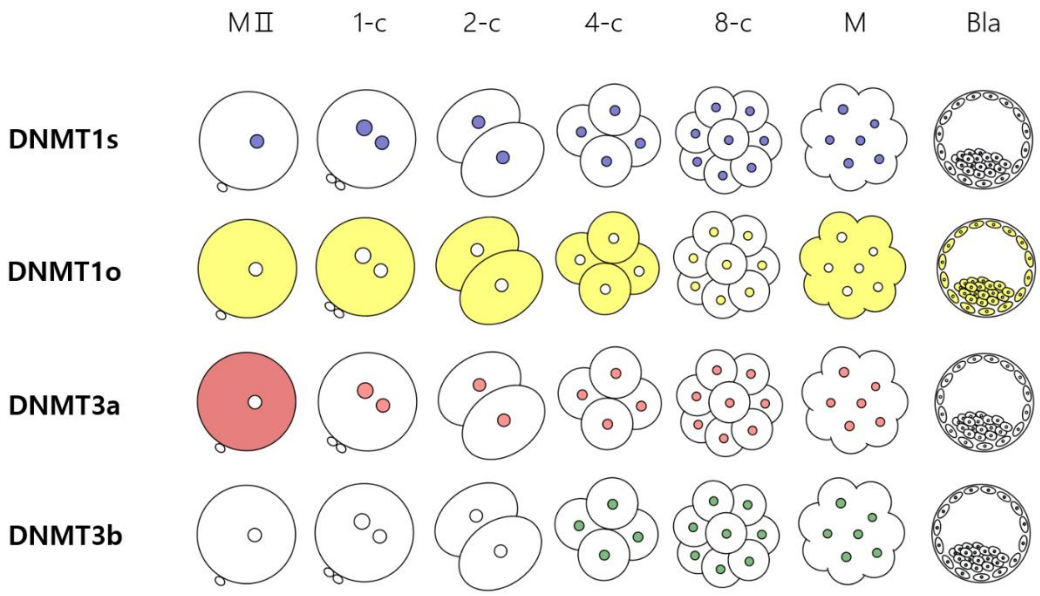

Figure 1. Diagram of expression of mouse DNMT in oocyte and early stage embryo

The DNMT enzymes are present in the mouse oocyte and early embryo, of which DNMT1s, DNMT1o, DNMT3a, and DNMT3b are mainly functions. The expression pattern of DNMT enzymes changes dynamically during oogenesis and embryogenesis. MⅡ ;MⅡ stage oocyte, 1-c ;1-cell stage embryo, 2-c ;2-cell stage embryo, 4-c ;4-cell stage embryo, 8-c ;8-cell stage embryo, M ;morula, Bla ;blastocyst.

MATERIALS AND METHODS

Experimental animals

All experimental animals were conducted according to the Guide for the Care and Use of Laboratory Animals published by the National Institute of Health (NIH). All animal procedures were approved by the Institutional Animal Care and Use Committee (IACUC) of Sungshin University (SSWIACUC-2023-010). Involving experiment animals were maintained under standard condition at Sungshin University. Diurnal rhythm kept under the 14L : 10D schedule with light-on at 6:00 and clean system. Bank vole PrP GPI KI(I109) (bvPrp GPI KI I109) mouse were on a C57BL/6 background. Genomic DNA was isolated from ear and the primer combination bvPrp GPI KI 1 (5′-GTATTAGAACTCACAGCCGTC-3′) and bvPrp GPI KI 2 (5′-CCTGAGTAACCGTAACACCACA-3′) was used to determine the genotype. 6-8-weeks-old female C57BL/6J mice was used as wild type.

Chemicals

Dimethyl sulfoxide (DMSO) purchased from Sigma (Sigma, D2650, Missouri, USA). DNMT1 inhibitors, N-phthalyl-L-tryptophan (RG108) purchased from Abcam (Abcam, ab141013, Cambridge, UK) and S-adenosylhomocysteine from Sigma (Sigma, A9384, Missouri, USA). maybridge (Myb1) was synthesized in Ambinter. 0.5% DMSO in media is used as a vehicle. 20 μM RG108 and 1 mM SAH, 0.5 μM, 1 μM, 10 μM, 20 μM Myb1 were used in the experiment.

Superovulation induction and embryo collection

Female C57BL/6 mice were superovulated by intraperitoneal injection 6 IU of PMSG followed 48 h later by intraperitoneal injection 6 IU hCG. And then these female mice were placed with stud males of the same strain. Mating status was confirmed by checking a presence of vaginal plug following morning. After 48 h, mouse embryos were collected 2-cell from oviduct by flushing with BWW medium containing 0.4% bovine serum albumin (BSA). To obtain the developmental embryos, 2-cell embryos were cultured for differenced time. After culture, 48 h (2-cell), 60 h (4-cell), 72 h (8-cell), 84 h (morula), 96 h (blastocyst), 120 h (hatching blastocyst), 144 h (hatched blastocyst) were collected for additional experiment. The collected samples were immediately stored at -196℃ liquid nitrogen in sterile tubes for real time quantitative PCR and RNA sequencing.

Total RNA extraction and First strand cDNA synthesis

Total RNAs were extracted from 10 pooled embryos using RNeasy®Micro Kit (QIAGEN, 74004, Germantown, USA) according to the manufacturer's instructions. First Strand cDNA Synthesis Kit (Agilent, 200820, California, USA) were used. Briefly, reaction reagents are 28 μl total RNA, 10 μl MMLV 5X buffer, 1 μl oligo dT primer (0.5 μg/μl), 1 μl random primer (0.1 μg/μl), 4 μl dNTP mix (100 mM). Reaction mixture was incubated at 65℃ for 5 min, placed the tube at RT for 5 min, and then added 4.5 μl DTT (100 mM), 2 μl M-MLV Reverse Transcriptase (Promega, M170B, Wisconsin, USA), 1 μl RNase block ribonuclease inhibitor (40 U/ml). The mixture was incubated at 42℃ for 1 hr and 70℃ for 15 min to terminate cDNA synthesis. And kept -20℃ before it used.

Real-time PCR analysis

For quantification of expression levels, transcripts of target genes were amplified using reverse transcript (RT)-PCR and the specific primers (Table 2). Quantification real time RT-PCR was performed using SYBR Premix Ex Taq™ (TaKaRa, RR420, Shiga, Japan) and AriaMx Real-time PCR System (Agilent, G8830A, California, USA). Information of the thermal cycle are in Table 1. Each reaction was run in triplicate and consisted of 1 μl cDNA. Dissociation curves were run on all reactions to ensure amplification of a single product with the appropriate melting temperature. The fold change in gene expression was calculated using the ΔΔCt method with the housekeeping gene, ribosomal protein, *36B4*, as the internal control.

Whole mount immunofluorescence of mouse embryo

Fixed embryos permeabilized with 0.5% PBST (PBS containing 0.5% Triton X-100) for 3 h. The embryos were blocked in PBS containing 1% BSA for 1 h at RT. After then, the embryos were incubated with primary antibody Prion (Table 3) diluted 1:200 in PBS containing 2% BSA at 4℃ overnight. After incubation, embryos were washed by transferring from drop to drop. The washed embryos were incubated with fluorescence 2nd antibody Alexa 594 diluted 1:200 in 0.5% PBST for 2 h at RT. The nuclear of embryos was staining with 4′ , 6-Diamidino-2-Phenylindole (DAPI) (Sigma, D9542, Missouri, USA) at 10 min. Dot slides were used for mounting. For negative control, we deleted primary antibodies. Finally, fluorescent images were analyzed by Zeiss LSM 700 laser microscope with ZEN software.

Sodium bisulfite genomic sequencing

Genomic DNAs were extracted from 10 pooled embryos using AllPrep® DNA/RNA/Protein Mini Kit (QIAGEN, 80004, Germantown, USA) and was then subjected to sodium bisulfite treatment using EpiJET Bisulfite Conversion Kit (thermo scientific, k1461, Massachusetts, USA) according to the manufacturer's instructions. Converted DNA was then amplified using bisulfite-specific PCR to obtain products for sequencing. PCR products were then gel-purified using a QIAquick® Gel Extraction Kit (Qiagen, 28704, Germantown, USA), and DNA methylation levels were quantified using colony sequencing. Briefly, purified products were inserted into T vector using AccuRapid^{TM}TA Cloning Kit (Bioneer, k-7170, Daejeon, Korea) and were transformed into competent TOP10 cell (Invitrogen, C404010, Massachusetts, USA). Colonies were then selected on lysogeny broth-ampicillin (100 μg/μl) agar using the IPTG/X-gal method, and plasmid DNA was subsequently extracted using QIAprep® Spin Miniprep Kit (Qiagen, 27104, Germantown, USA). Finally, sequencing was performed with BigDye Terminator v3.1 Cycle Sequencing Kit and applied Biosystems 3730xl DNA Analyzer. Sequencing results were analyzed using a quantification tool for DNAme analysis, QUMA.

Embryo transfer

Estrus stage female CD1 mice, mated with vasectomized CD1 males, were used as recipients for embryo transfers. Mating was confirmed by the presence of a vaginal plug the following morning. Blastocyst transfers were performed 2.5 days post coitum. Early blastocysts of similar morphology were then transferred to the uterus (n = 8 per horn) of pseudo-pregnant recipients.

RNA-seq library preparation and sequencing data processing

To generate RNA-seq library, 50 embryos were used per reaction. The sequencing libraries were constructed using the TruePrep Index Kit V2 for Illumina (Vazyme Biotech, TD502-01) according to the manufacturer's instruction. All libraries were sequenced on the Illumina NovaSeq platform in 101-bp paired-end mode at the Rokit Genomics Company (Seoul, Korea). Raw data files were generated through sequencing and processed into information of read quality, total base number, total read number, GC content through quality control. And low-quality reads, adapter sequence and PCR-duplicated reads were removed by adapter trimming Trimmomatic V 0.38. Preprocessing reads were aligned using HISAT2 V 2.1.0. And gene expression profile matrixes were generated using StringTie V 2.1.3b by sample, by gene, by quantification. Then Differentially expression (DE) and downstream analysis conducted using DESeq2 V 1.38.0.

Statistics

The results represent means ± SED. The data were analyzed using one-way analysis of variance (ANOVA) and t-test between control and experimental group. In all cases, values of $p<0.05$ were deemed to indicate statistical significance.

Table 1. Real-time RT-PCR Thermal cycler schedule

Step		Temperature (℃)	Time	cycles
Hold		94	30 min	1
3 steps PCR	Denaturation	95	1 min	45
	Annealing	59	30 sec	
	Extension	72	1 min	
Dissociation	Denaturation	95	15 sec	1
	Annealing	60	30 sec	
	Extension	95	15 sec	
Hold		4	Indefinitely	1

Table 2. Primer sequences for quantitative real-time PCR

Gene	Symbol	NCBI gene reference		Primer sequence (5'-3')	Amplified length (bp)
Endogenous retroviral sequence 4	***MuERV-L (Erv4)***	NM_001166206.1	S	TGGTGGTCGAGATGGAGGTTA	231
			AS	CCGTGAATGGTGGTTTTAGCA	
Caudal type homeobox2	***Cdx2***	NM_007673.3	S	CCCTAGGAAGCCAAGTGAAAACCA	265
			AS	TTGGCTCTGCGGTTCTGAAAC	
SRY-box transcription factor 2	***Sox2***	NM_011443.4	S	TGAACGCCTTCATGGTATGGTC	240
			AS	TCCTTCTTCATGTGCGTCTTGG	
Gap junction protein, beta 1	***Cx32 (Gjb1)***	NM_001302496.1	S	TCCGGCATCTGCATTATCCT	287
			AS	AGCATCGGTCGCTGTTTTCA	
Desmocollin2	***Dsc2***	NM_001317363.1	S	AATGACAACCTGCCCACGTT	322
			AS	CTGTGCTCATGGGTGACTTTGA	
E-cadherin	***Cdh1***	NM_009864.3	S	GATTCAGTTCCGAGGTCTACACCTT	265
			AS	GGAGCTTTAGATGCCGCTTCACT	
Yes1 associated transcriptional regulator	***Yap1***	NM_001171147.1	S	GACTTGGAGGCGCTCTTCAAT	243
			AS	GAACATGCTGTGGAGTCAGAGCT	
POU domain, class 5, transcription factor 1	***Oct4 (Pou5f1)***	NM_001252452.1	S	CGTGAAGTTGGAGAAGGTGGAA	211
			AS	GCCGCAGCTTACACATGTTCTT	

Nanog homeobox	***Nanog***	NM_001289828.1	S	TCTGGGAACGCCTCATCAAT	241
			AS	TGAGAGAACACAGTCCGCATC	
DNA methyltransferase 1	***Dnmt1***	NM_001199431.2	S	AGCGTTGTGGTGGATGACAAGAA	243
			AS	TGTGGTATGGGCTCTGCTCAGGTT	
DNA methyltransferase 3A	***Dnmt3a***	NM_001271753.2	S	CATCTGTAACCCCAGCCCTTTT	230
			AS	TTTACTCGCTAACCCAGAGCCT	
DNA methyltransferase 3B	***Dnmt3b***	NM_001003960.5	S	ACCGGTCATCAGACACCTGTTT	194
			AS	ACTGAGCAGGAGAAAGCTGAGGTA	
Imprinted maternally expressed transcript	***H19***	NR_130973.1	S	ACCATGGGATCCAGCAAGAA	204
			AS	TGCACTGCCCTTCTTTTCCA	
Small nuclear ribonucleoprotein N	***Snrpn***	NM_001082961.2	S	AAGGCAATGCAGCAACCAAG	225
			AS	CCAAGAGGGAATCACAGCAGAT	
Prion protein	***Prnp***	NM_001278256.1	S	ATCATGGCGAACCTTGGCTACT	243
			AS	AACTACCACCATGAGGTTGTCCC	
Methyl-Prion protein	***Prnp***	NM_001278256.1	S	GGAGCATTGGGTACTGGATCAG	544
			AS	TGCTGAGCTGTGAATCTGGC	
60S acidic ribosomal protein P0	***Rplp0 (36B4)***	NM_007475	S	CGACCTGGAAGTCCAACTACTTCCT	303
			AS	GCACCTTATTGGCCAACAGCAT	

Table 3. Antibody information

Antibody	Description	Cat #	Company
Prion	Mouse monoclonal	MA1-750	Invitrogen

RESULTS

Effects of the of Myb1 on early stage embryo development

So far, it has been studied that the DNMT1 modulators have anticancer activity and causes the reactivation of the tumor suppressor gene and have been shown positive effect on embryo development. To test whether myb1 could improve the early development of mouse embryo in vitro culture, we treated the 2-cell stage embryos with different concentrations of myb1 and evaluated the developmental rates from 60 h (4-cell) (Table 4). There was no difference at developmental rate between 60 h (4-cell) and 72 h (8-cell). But, In 10 μM myb1, ≥hatching blastocyst (120 h) rate (40.00%) was significantly increased than vehicle group (22.44%). There was no significant increase in the remaining concentration groups. Therefore, 10 μM myb1 was selected in this study.

Table 4. Developmental rate of early mouse embryos

	Developmental rate (%)					
	60h (≥4-cell)	**72h** (≥8-cell)	**84h** (≥Morula)	**96h** (≥Blastocyst)	**120h** (≥Hatching Blastocyst)	**144h** (≥Hatched Blastocyst)
vehicle	93.87	92.85	89.87	72.44	22.44	35.71
0.5μM Myb1	89.47	94.73	92.85	65.78	18.42	30.26
1μM Myb1	91.46	98.78	100	70.73	36.58	35.36
10μM Myb1	96.47	96.47	100	72.94	40.00*	37.65
20μM Myb1	95.61	96.49	97.36	72.80	38.59	28.07

After 2-cell embryos were cultured with DNMT1modulator, Myb1, developmental rate of ≥4-cell (post hCG 60 h), ≥8-cell (72 h), ≥morula (84 h), ≥blastocyst (96 h), ≥hatching blastocyst (120 h), ≥hatched blastocyst (144 h) embryos was examined.

*, $p < 0.05$ compared with vehicle

Developmental rate of WT early embryos under different DNMT1 modulators.

The possible roles of Myb1 was evaluated with comparing in developmental capacity of embryos (Table 5). 2-cell embryos were treated with DNMT1 inhibitors SAH, RG108. The development to 72 h (8-cell) was similar between groups. But showed difference after 84 h post hCG (Morula stage). Developmental rate of embryos treated with SAH was significantly decreased of ≥blastocyst (96 h), and ≥hatched blastocyst (144 h) than vehicle and myb1. Developmental rate of embryos treated with RG108 was similar with vehicle. In ≥hatching blastocyst (120 h), developmental rate was increased but not significant.

Table 5. Developmental rate of WT early embryos

	Developmental rate (%)					
	60h (≥4-cell)	**72h** (≥8-cell)	**84h** (≥Morula)	**96h** (≥Blastocyst)	**120h** (≥Hatching Blastocyst)	**144h** (≥Hatched Blastocyst)
vehicle	93.87	92.85	89.87	72.44	22.44	35.71
10μM Myb1	96.4	96.47	100	72.94	40[a]	37.65
1mM SAH	91.17	89.7	92.68	42.64[ab]	17.64[ab]	14.71[ab]
20μM RG108	92.42	95.45	87.8	74.24	33.33	28.79

After 2-cell embryos culture with DNMT1 inhibitors, developmental rate of ≥4-cell (post hCG 60 h), ≥8-cell (72 h), ≥morula (84 h), ≥blastocyst (96 h), ≥hatching blastocyst (120 h), ≥hatched blastocyst (144 h) embryos was examined.

a, $p < 0.05$ compared with vehicle

b, $p < 0.05$ compared with 10 μM Myb1

Developmental rate of KI early embryos under different DNMT1 modulators

As with the results of WT, development rate had a gradual decrease in embryo treated with SAH from morula (84 h) and a significant decrease compared to the vehicle and Myb1 at 96 h,120 h and 144 h. Embryo treated with Myb1 was similar to the developmental rate of embryo treated with vehicle by 144 h (Table 6). On the other hand, embryo treated with RG108 increased the developmental rate compared to vehicle. In particular, it increased significantly at ≥hatching blastocyst (120 h).

Table 6. Developmental rate of KI early embryos

	Developmental rate(%)					
	60h (≥4-cell)	**72h** (≥8-cell)	**84h** (≥Morula)	**96h** (≥Blastocyst)	**120h** (≥Hatching Blastocyst)	**144h** (≥Hatched Blastocyst)
vehicle	98.41	95.28	89.67	83.96	55.66	41.50
10μM Myb1	98.36	97.85	98.92	78.49	54.83	55.91
1mM SAH	97.70	86.92[b]	72.92	60[ab]	36.15[ab]	26.15[ab]
20μM RG108	96.72	95.14	98.05	94.17	85.39[a]	60.19

After 2-cell embryos culture with DNMT1 inhibitors, developmental rate of ≥4-cell (post hCG 60 h), ≥8-cell (72 h), ≥morula (84 h), ≥blastocyst (96 h), ≥hatching blastocyst (120 h), ≥hatched blastocyst (144 h) embryos was examined.

a, $p < 0.05$ compared with vehicle

b, $p < 0.05$ compared with 10 μM Myb1

Expression level of potency and competency markers on WT early stage embryo after DNMT1 modulators treatment

We investigated the expression levels of nine genes affecting the development in DNMT1 inhibitor-treated embryos (Figure 2). *MuERV-L* as a totipotency marker, *Cdx2* and *Sox2* as TE lineage-related markers, *Cx32* and *Dsc2* as polarity-related markers, *Yap* and *Cdh1* as forming related markers, and *Pou5f1* and *Nanog* as pluripotent-related markers were used. *MuERV-L* mRNA levels were shown a similar pattern between oocytes and embryos treated vehicle and myb1. At the 4-cell stage embryo of SAH-treated group, it increased compared to the vehicle, but there was no significant difference. But, The RG108 treatment group showed a higher pattern than the vehicle group except for the morula stage and was significantly higher in the hatching blastocyst stage embryos (Fig. 2A). In *Cdx2*, vehicle and myb1 treatment groups and the SAH and RG108 treatment groups showed similar patterns as a whole. In 8-cell stage, SAH and RG108 treatment groups were decreased, and SAH showed significant levels (Fig. 2B). The *Sox2* mRNA levels of the vehicle and myb1-treated groups were very similar across all stages, and the RG108-treated groups were similar except for the hatching blastocyst stage. However, the SAH treatment group showed an overall decreasing pattern and was significant in hatching and hatched blastocyst stage (Fig. 2C). The *Cx32* mRNA levels in vehicle, myb1, and RG108-treated groups were similar, but significantly increased in blastocyst stage embryo in SAH-treated groups (Fig. 2D). There were showed similarity in *Dsc2* between all groups, but significantly reduced in the blastocyst stage of the SAH-treated group (Fig. 2E). There was no difference in the mRNA levels of *Yap* and *Cdh1* in all groups (Fig. 2F, G). In *Pou5f1*, the mRNA level of the myb1-treated group was significantly increased after morula stage compared to the vehicle (Fig. 2H). Similarly, in mRNA level of *Nanog*, myb1 showed higher expression compared to the other groups but was not significant (Fig. 2I). Overall, embryos cultured by SAH treatment showed a severe decrease in the development rate from

≥blastocyst (96 h), especially in TE lineage and polarity-related genes. This suggests that culture with 1 mM SAH treatment on an early stage embryo has a bad effect on forming a blastocyst. On the other hand, 10 μM myb1 is treated and the developmental rate increases in the ≥hatching blastocyst (120 h) stage, which is seen as the effect of the increase in the expression of pluripotency-related genes. Similar to the results of WT, SAH-treated embryos showed defects in TE lineage, polarity-related genes from 72 h (8-cell) and 84 h (morula), and increased expression of pluripotency-related genes in Myb1 treated embryos.

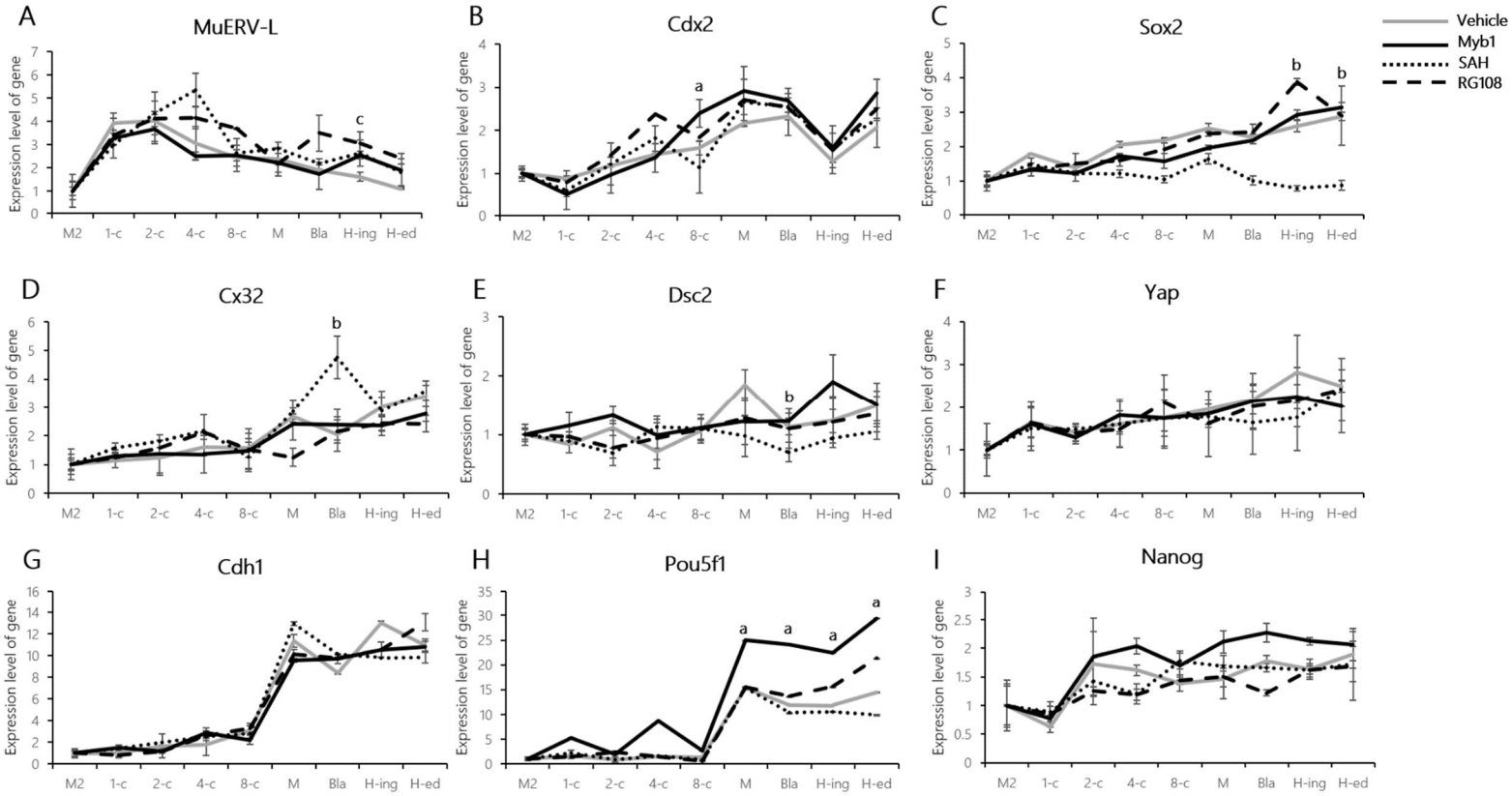
A
MuERV-L
B
Cdx2
C
Sox2
D
Cx32
E
Dsc2
F
Yap
G
Cdh1
H
Pou5f1
I
Nanog
Expression level of gene
M2
1-c
2-c
4-c
8-c
M
Bla
H-ing
H-ed
Vehicle
Myb1
SAH
RG108

Figure 2. Profile of potency and competency markers in DNMT1 inhibitors treatment on WT early embryos

Relative expression levels of *MuERV-L* mRNA (A), *Cdx2* mRNA (B), *Sox2* mRNA (C), *Cx32* mRNA (D), *Dsc2* mRNA (E), *Yap* mRNA (F), *Cdh1* mRNA (G), *Pou5f1* mRNA (H) and *Nanog* mRNA (I) expression level changes in wild type early stage embryos were cultured with each DNMT1 inhibitors. Gray solid line is vehicle group, black solid line is myb1 group, black dotted line is SAH group and black dashed line is RG108 group. Gene expression was calculated using the ΔΔCt method with the *36B4*, as the internal control. a: $p < 0.05$ (vehicle to myb1), b: $p < 0.05$ (vehicle to SAH), c: $p < 0.05$ (vehicle to RG108). Data are represented as the mean ±SEM.

Expression level of potency and competency markers on KI early stage embryo after DNMT1 modulators treatment

In KI mice, we also examined the mRNA expression of potency and competency related genes to investigate the effects of DNMT1 inhibitors on early embryo development (Figure 3). *MuERV-L* levels of 2-cell embryo treated Myb1 was decreased but, embryo treated SAH, RG108 were increased than vehicle. It was not significant (Fig. 3A). Levels of *Cdx2* increased but not significantly in 120 h (hatching blastocyst) embryo treated with Myb1, RG108, and SAH decreased (Fig. 3B). In *Sox2*, it increased in Myb1, Rg108 treated embryo compared to vehicle from 96 h (blastocyst) but decreased significantly from 84 h (morula) in SAH-treated embryo (Fig. 3C). When treated with RG108, the *Cx32* level was significantly reduced at 60 h (4-cell), continued to be low, and showed a similar pattern to the rest of the vehicle (Fig. 3D). In *Dsc2*, the embryo treated with SAH decreased from 60 h (4-cell) and was significantly reduced in 72 h (8-cell), 96 h (blastocyst), 120 h (hatching blastocyst), and 144 h (hatched blastocyst) (Fig. 3E). There was no difference in the mRNA levels of *Yap* and *Cdh1* in all groups (Fig. 3F, G). In *Pou5f1*, the mRNA level of the myb1-treated group was increased after morula stage compared to the vehicle and it was significantly increased at 120 h (hatching blastocyst). However, it was significantly reduced at 96 h (blastocyst) and 144 h (hatched blastocyst) in SAH-treated embryos (Fig. 3H). *Nanog* mRNA levels in embryos treated with all inhibitors showed similar pattern (Fig. 3I).

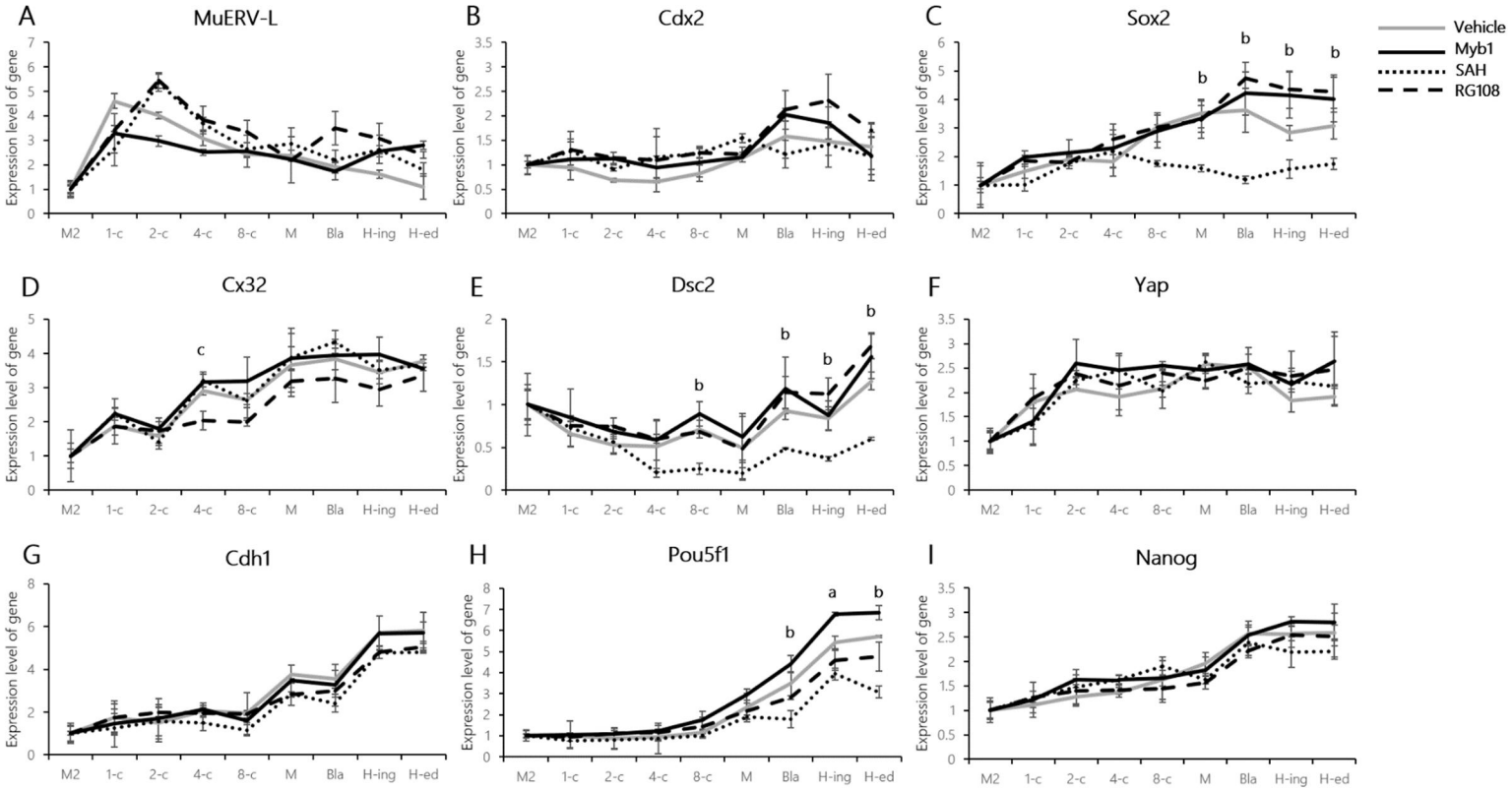
A
MuERV-L
B
Cdx2
C
Sox2
D
Cx32
E
Dsc2
F
Yap
G
Cdh1
H
Pou5f1
I
Nanog
Expression level of gene
M2
1-c
2-c
4-c
8-c
M
Bla
H-ing
H-ed
Vehicle
Myb1
SAH
RG108

Figure 3. Profile of potency and competency markers in DNMT1 inhibitors treatment on KI early embryos

Relative expression levels of *MuERV-L* mRNA (A), *Cdx2* mRNA (B), *Sox2* mRNA (C), *Cx32* mRNA (D), *Dsc2* mRNA (E), *Yap* mRNA (F), *Cdh1* mRNA (G), *Pou5f1* mRNA (H) and *Nanog* mRNA (I) expression level changes in wild type early stage embryos were cultured with each DNMT1 inhibitors. Gray solid line is vehicle group, black solid line is myb1 group, black dotted line is SAH group and black dashed line is RG108 group. Gene expression was calculated using the ΔΔCt method with the *36B4*, as the internal control. a: $p< 0.05$ (vehicle to myb1), b: $p< 0.05$ (vehicle to SAH), c: $p< 0.05$ (vehicle to RG108). Data are represented as the mean ±SEM.

Expression level of imprinted genes and DNA methyltransferase genes on WT early stage embryo after DNMT1 modulators treatment

H19 gene is imprinted in mammals and transcribed from maternal allele. On the other hand, *Snrpn* is a maternal imprinting gene, and these transcripts are paternally expressed. The expression level of imprinted genes and DNA methyltransferase genes is also vital for nuclear reprogramming. When mRNA levels of *H19* and *Snrpn* genes were compared in embryo cultured by treatment with DNMT1 inhibitors, no significant difference was found between each treatment group (Fig. 4A, B). At the mRNA level of *Dnmt1*, the three DNMT inhibitor treated groups tended to be lower than the vehicle, but not significant (Fig. 4C). The *Dnmt3a* mRNA level showed a similar pattern without significant differences between groups (Fig. 4D). And at the *Dnmt3b* mRNA level, there was little difference from the vehicle in the SAH-treated embryos, and the myb1 and RG108-treated groups showed a slightly decreasing pattern after the morula stage (Fig. 4E). Therefore, it is suggested that treating 10 μM myb1, 1 mM SAH, and 20 μM RG108 during mouse early embryo culture does not affect the imprinted genes and does not significantly change the mRNA levels of DNA methyltransferase genes.

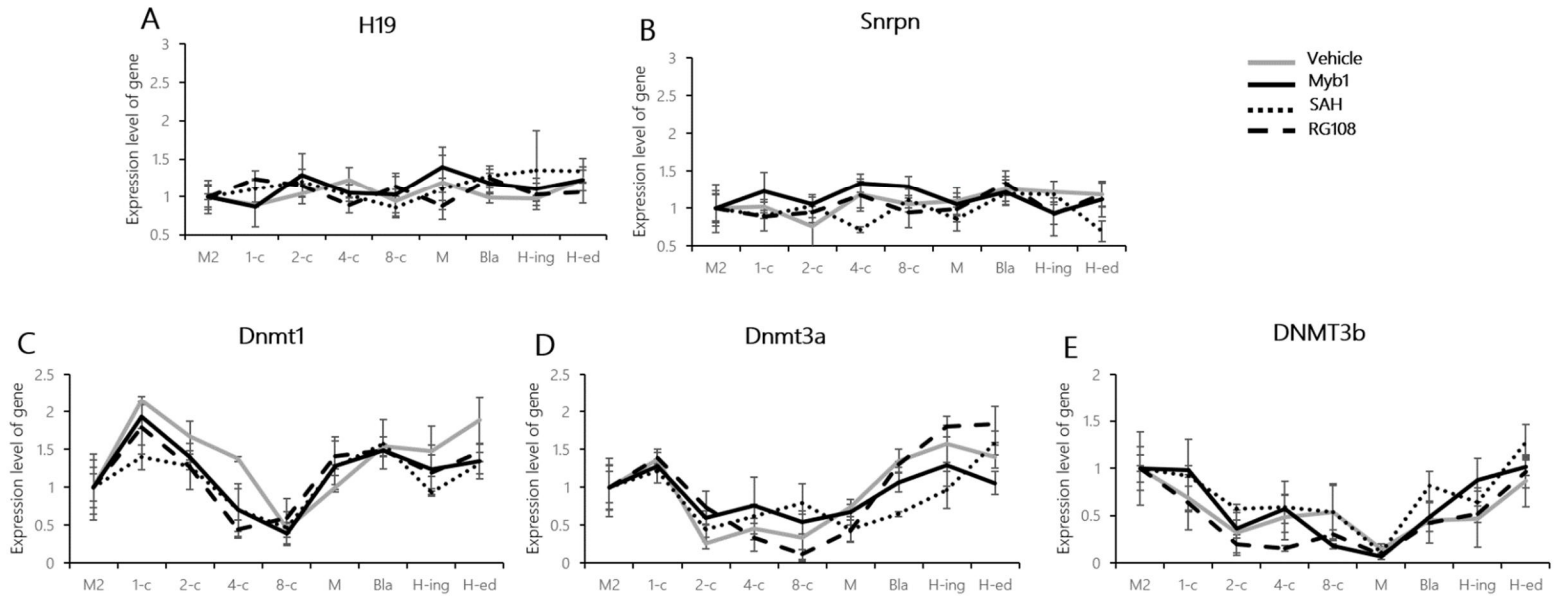
A
H19
B
Snrpn
Vehicle
Myb1
SAH
RG108
Expression level of gene
M2
1-c
2-c
4-c
8-c
M
Bla
H-ing
H-ed
C
Dnmt1
D
Dnmt3a
E
DNMT3b

Figure 4. Profiles of imprinted genes and DNA methyltransferase genes after DNMT1 inhibitors treatment on WT early embryos

Relative *H19* mRNA (A), *Snrpn* mRNA (B), *Dnmt1* mRNA (C), *Dnmt3a* mRNA (D) and *Dnmt3b* mRNA (E) expression level changes in wild type early stage embryos cultured with each DNMT1 inhibitors. Gray solid line is vehicle group, black solid line is myb1 group, black dotted line is SAH group and black dashed line is RG108 group. Gene expression was calculated using the ΔΔCt method with the *36B4*, as the internal control. a: $p < 0.05$ (vehicle to myb1), b: $p < 0.05$ (vehicle to SAH), c: $p < 0.05$ (vehicle to RG108). Data are represented as the mean ±SEM.

Expression level of imprinted genes and DNA methyltransferase genes on KI early stage embryo after DNMT1 modulators treatment

When the expression of imprinted genes and DNMT family genes was examined in KI mice, the results were similar to WT. *H19* and *Snrpn* were compared in embryo cultured by treatment with DNMT1 inhibitors, no significant difference was found between each treatment group (Fig. 5A, B). At the mRNA level of *Dnmt1*, the three DNMT inhibitor treated groups tended to be lower than the vehicle, but not significant (Fig. 5C). The *Dnmt3a* and *Dnmt3b* mRNA level showed a similar pattern without significant differences between groups (Fig. 5D, E). Therefore, it is suggested that treating 10 μM myb1, 1 mM SAH, and 20 μM RG108 during KI mouse early embryo culture does not affect the imprinted genes and does not significantly change the mRNA levels of DNA methyltransferase genes. These results suggest that DNMT1 inhibitors affect early embryo development without altering the expression of imprinted genes and DNMT family genes.

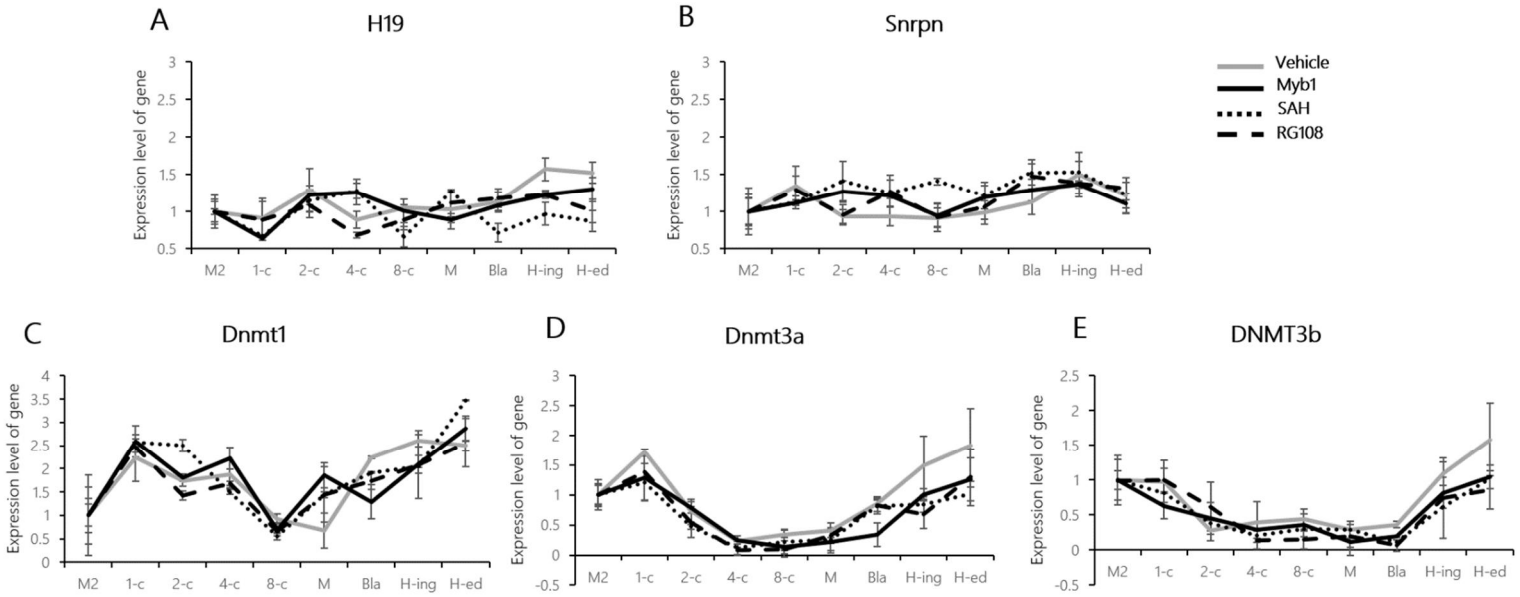
A
H19
B
Snrpn
Vehicle
Myb1
SAH
RG108
Expression level of gene
M2
1-c
2-c
4-c
8-c
M
Bla
H-ing
H-ed
C
Dnmt1
D
Dnmt3a
E
DNMT3b

Figure 5. Profiles of imprinted genes and DNA methyltransferase genes after DNMT1 inhibitors treatment

Relative *H19* mRNA (A), *Snrpn* mRNA (B), *Dnmt1* mRNA (C), *Dnmt3a* mRNA (D) and *Dnmt3b* mRNA (E) expression level changes in wild type early stage embryos cultured with each DNMT1 inhibitors. Gray solid line is vehicle group, black solid line is myb1 group, black dotted line is SAH group and black dashed line is RG108 group. Gene expression was calculated using the ΔΔCt method with the *36B4*, as the internal control. a: $p < 0.05$ (vehicle to myb1), b: $p < 0.05$ (vehicle to SAH), c: $p < 0.05$ (vehicle to RG108). Data are represented as the mean ±SEM.

Expression pattern of *Prnp* on WT mouse early embryo development after DNMT1 modulators treatment

To analyze the *Prnp* Gene expression pattern of preimplantation embryos from MⅡ stage oocytes to hatched embryos, mRNA was analyzed by quantitative PCR and protein was analyzed by whole-mount embryo immunofluorescence. When analyzing the *Prnp* mRNA pattern of oocytes and embryos, it increased slightly at 1-cell stage, then decreased to morula stage, and then increased again from blastocyst stage (96 h), and all DNMT1 inhibitors treatment groups showed similar patterns (Fig. 6A). Also, we checked the protein level of the detected PrP. Protein expression level can confirm localization in early stage embryo. PrP expression is strongly expressed in 2-cell, and continues to be expressed from morula stage similar to mRNA expression (Fig 6B). And from 2-cell to hatching blastocyst (120 h), Prion protein is localized in cytoplasm. However, PrP expression at morula was significantly decreased than vehicle group in embryos treated DNMT1 inhibitors. In 96h (blastocyst stage), intensity of PrP rises again and then slightly decreases in 120h (hatching blastocyst) (Fig 6C). These data indicate that DNMT inhibitors affect PrP expression in morula stage (84 h) embryo.

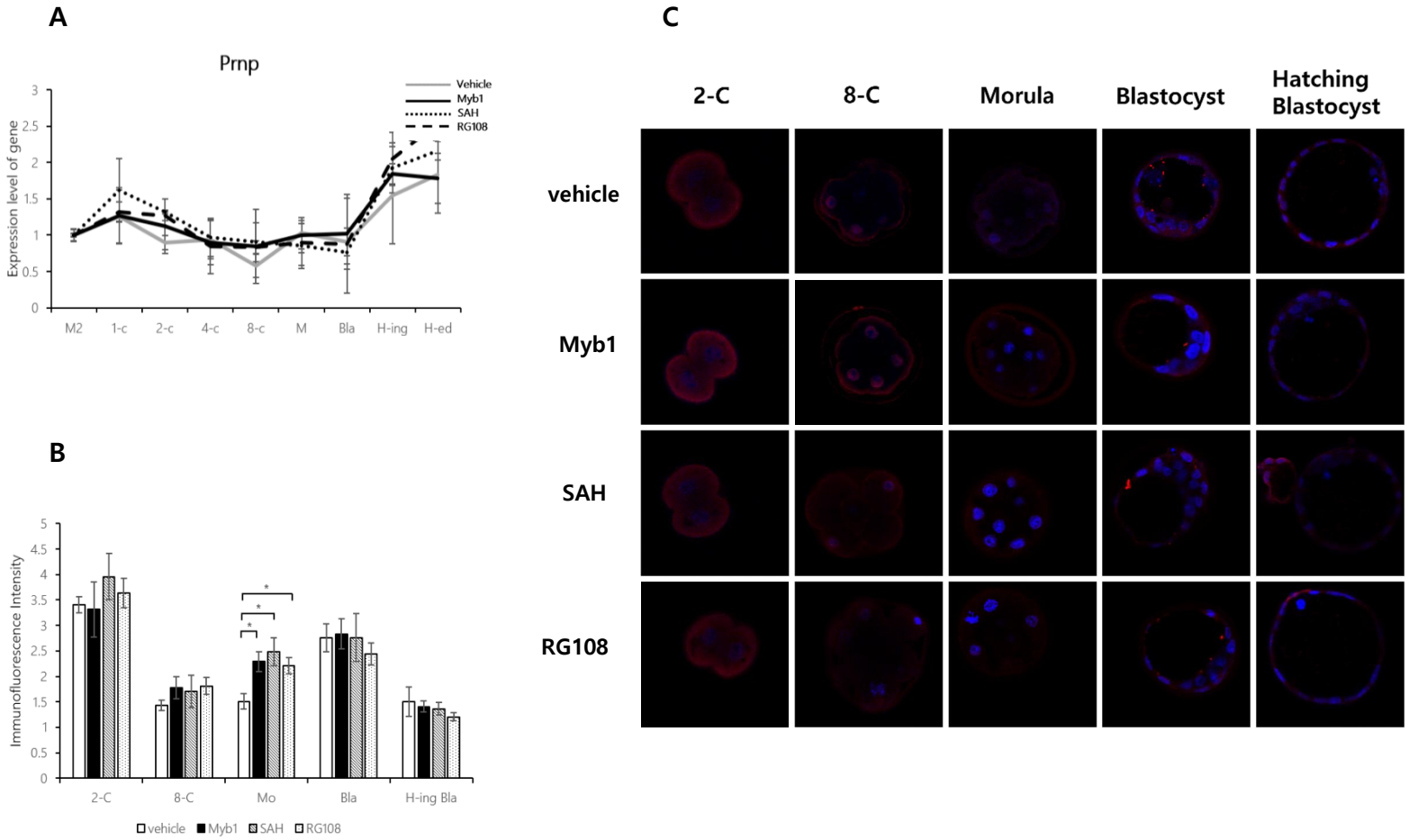
A
Prnp
Vehicle
Myb1
SAH
RG108
Expression level of gene
3
2.5
2
1.5
1
0.5
0
M2
1-c
2-c
4-c
8-c
M
Bla
H-ing
H-ed
B
Immunofluorescence Intensity
5
4.5
4
3.5
3
2.5
2
1.5
1
0.5
0
2-C
8-C
Mo
Bla
H-ing Bla
vehicle
Myb1
SAH
RG108
C
2-C
8-C
Morula
Blastocyst
Hatching Blastocyst
vehicle
Myb1
SAH
RG108

Figure 6. Expression of *Prnp* on WT early embryo development

(A) mRNA expression of *PRNP gene*, (B) Whole-mount immunofluorescence images of preimplantation embryos stained with antibody against Prion protein (red). DNA was counterstained with DAPI (blue). *: $p<0.05$(vehicle to each group). Data are represented as the mean ±SEM. Magnification X630.

Expression pattern of *Prnp* on KI mouse early embryo development after DNMT1 modulators treatment

When *Prnp* mRNA was analyzed in KI mice, it showed an increase in DNMT1 inhibitors treated embryos starting at 96h (blastocyst) (Fig 7A). In 1-cell embryos, vehicle and Myb1 showed high levels, but in embryos treated with SAH and RG108, the levels were lower than vehicle, although not significantly different. *Prnp* levels were significantly increased in embryos treated with RG108 at 84 h (morula). Then, PrP levels were examined in embryos by embryo whole mount immunofluorescence (Fig 7C). PrP expression was located in the cytoplasm throughout and showed strong expression than in WT, and increased at 96 h (blastocyst) and then decreased again at 120 h (hatching blastocyst). At 84 h (morula), in embryos treated with RG108, the intensity was inductively increased compared to vehicle, similar to the mRNA results (Fig 7B). This data suggests that DNMT1 inhibitor affects *Prnp* expression.

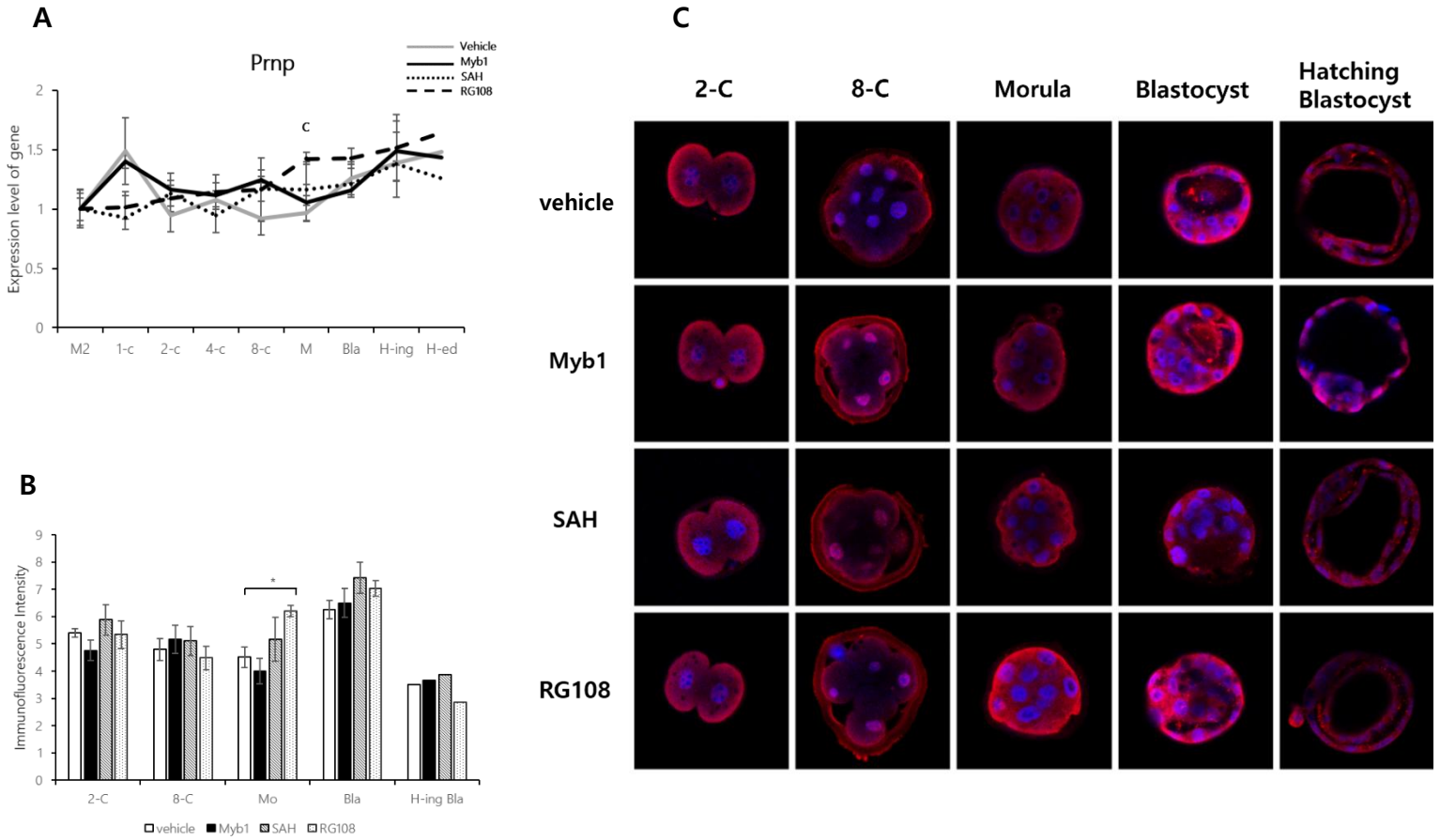
A
Prnp
Vehicle
Myb1
SAH
RG108
c
Expression level of gene
2
1.5
1
0.5
0
M2
1-c
2-c
4-c
8-c
M
Bla
H-ing
H-ed
B
Immunofluorescence Intensity
9
8
7
6
5
4
3
2
1
0
*
2-C
8-C
Mo
Bla
H-ing Bla
vehicle
Myb1
SAH
RG108
C
2-C
8-C
Morula
Blastocyst
Hatching Blastocyst
vehicle
Myb1
SAH
RG108

Figure 7. Expression of *Prnp* on KI early embryo development

(A) mRNA expression of *PRNP gene*, (B) Whole-mount immunofluorescence images of preimplantation embryos stained with antibody against Prion protein (red). DNA was counterstained with DAPI (blue). *: $p<0.05$(vehicle to each group). Data are represented as the mean ±SEM. Magnification X630.

Effect of DNA methylation pattern of CpG island in *Prnp* promotor region after DNMT1 modulators treatment on WT early embryo

In mouse, the *Prnp* gene exists within chromosome 2 and consists of three exons. The *Prnp* region we targeted in this study is the as the promoter region (428 bp upstream the transcription start site (TSS)) between exons 1 and 2. Among them, the methylation pattern was investigated in a region of 544 bp containing 38 CpG sites in a region known as CpG island (CGI). Bisulfite sequencing was performed whether DNMT1 inhibitors change the DNA methylation pattern in *Prnp* gene in mouse early embryo. We analyzed methylation pattern in 2-cell, morula (84 h), hatching blastocyst (120 h), hatched blastocyst (144 h) stage embryos (Fig. 8). However, all stages and treatment groups showed the result of the hypomethylated state.

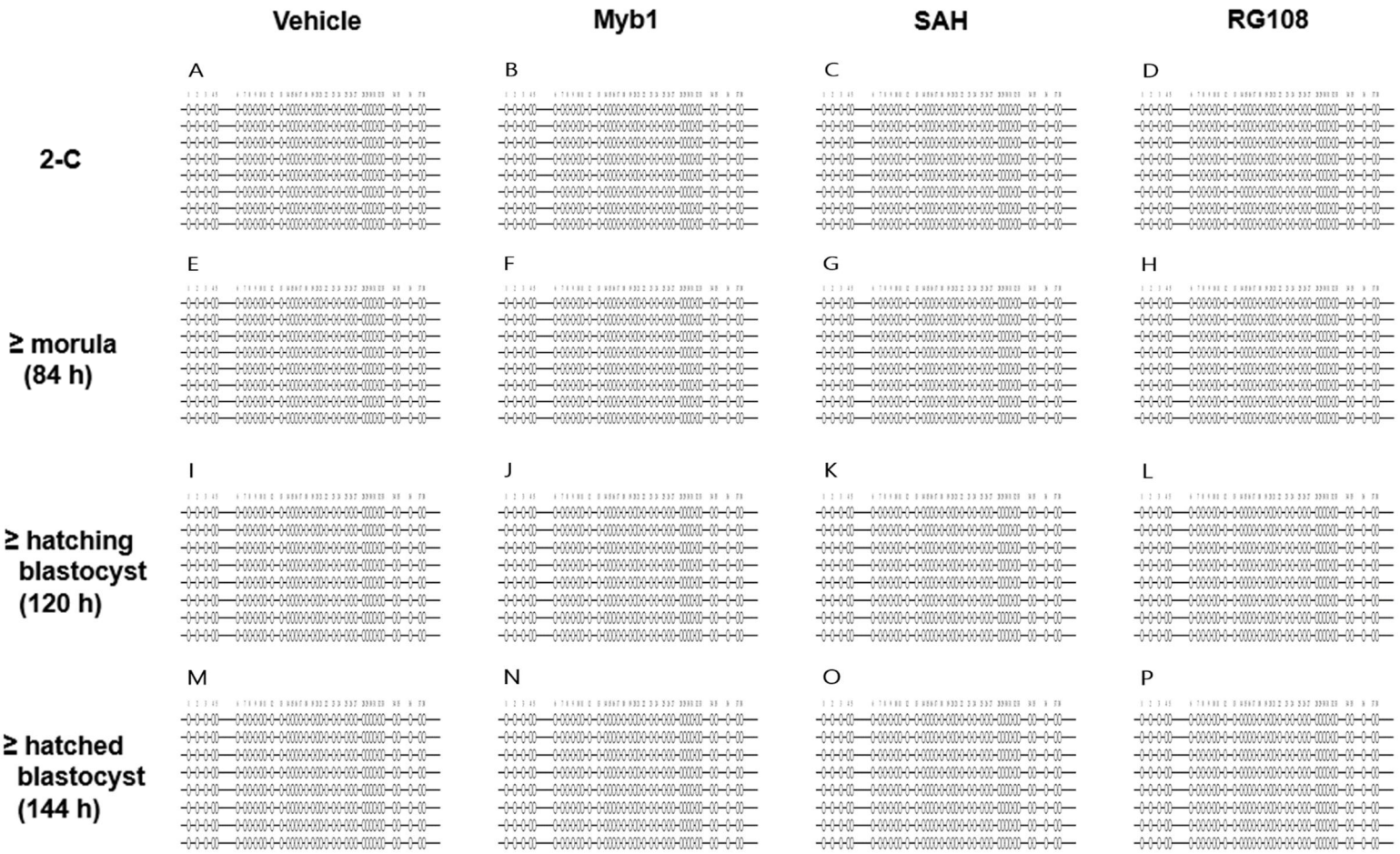
Vehicle
Myb1
SAH
RG108
2-C
≥ morula (84 h)
≥ hatching blastocyst (120 h)
≥ hatched blastocyst (144 h)
A
B
C
D
E
F
G
H
I
J
K
L
M
N
O
P

Figure 8. Bisulfite sequencing on promotor region in preimplantation WT mouse embryo after DNMT1 inhibitors treatment

Schematics indicate the position of analyzed CpG islands in promoter regions. (white circles) unmethylated CpGs. Within a group, 8 random colonies from each group were used for this assay.

Effect of DNA methylation pattern of CpG island in *Prnp* promotor region after DNMT1 modulators treatment on KI early embryo

We performed bisulfite sequencing on the CpG island of the *Prnp* gene promoter region in KI mice (Figure 9). As in WT, there was no change in all stages and DNMT1 inhibitor treated embryos, and all remained hypomethylated state. These results suggest that Myb1, SAH, and RG108 do not affect methylation at CpG sites in the *Prnp* gene promoter region. And it means that DNMT1 inhibitor regulates expression through other regions without affecting the DNA methylation pattern at the *Prnp* gene CpG site.

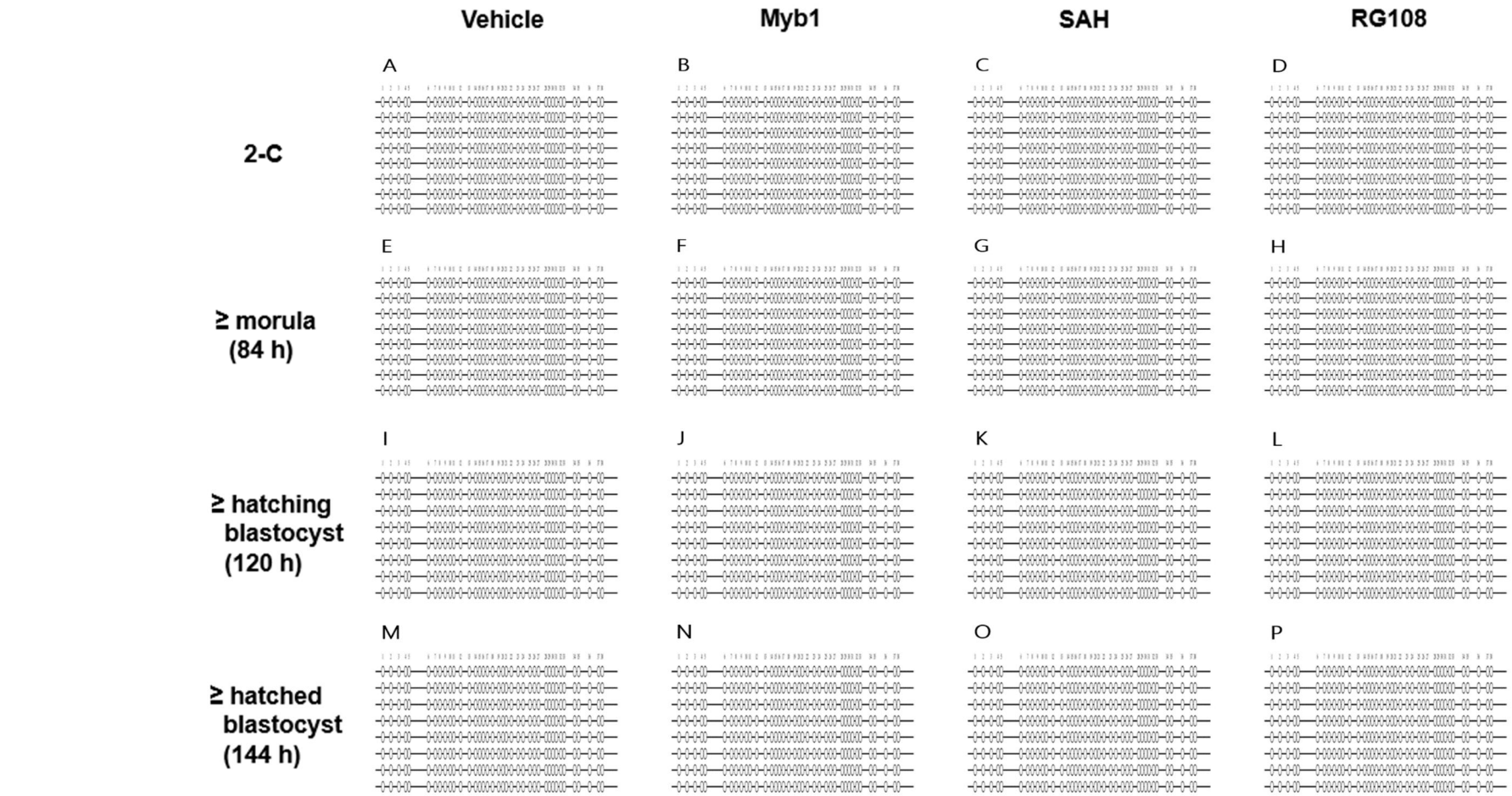
Vehicle
Myb1
SAH
RG108
2-C
≥ morula (84 h)
≥ hatching blastocyst (120 h)
≥ hatched blastocyst (144 h)
A
B
C
D
E
F
G
H
I
J
K
L
M
N
O
P

Figure 9. Bisulfite sequencing on promotor region in preimplantation KI mouse embryo after DNMT1 inhibitors treatment

Schematics indicate the position of analyzed CpG islands in promoter regions. (white circles) unmethylated CpGs. Within a group, 8 random colonies from each group were used for this assay.

Effect of different DNMT1 modulators on the implantation and litter size

In order to evaluate the effects of DNMT modulators after implantation of embryos which cultured during cleavage in vitro with DNMT modulators. Embryo transfer was performed post hCG 96 h blastocyst stage. When the embryo cultured by myb1 treatment was transferred, the ratio of the number of pups born was significantly higher than that of the vehicle group. On the other hand, in the SAH-treated group, the proportion was significantly reduced, and the RG108-treated group showed a similar pattern to the vehicle (Table 7). Therefore, it can be seen that mouse embryo cultured by treating myb1 can have a positive effect on development potency even after implantation.

Table 7. Live birth rate of the DNMT1 inhibitor treated embryos during cleavage

	Embryo transfer			
	vehicle	**myb1**	**SAH**	**RG108**
No. of transferred embryos	180	102	64	116
pup number	22	19	4	15
ET percentage	11.87%	16.43%[a]	6.25%[b]	11.61%

After embryo transfer, we compared the number of pups born compared to the number of embryos that were treated and in vitro-cultured by DNMT inhibitors.

a, $P < 0.05$ significantly increased compared to vehicle

b, $P < 0.05$ significantly reduced compared to vehicle

Organ weights of 5 weeks old mice which were developed from the DNMT1 modulator treated embryos

To investigate whether pups born after embryo transfer have defects in their development, we compared the organ weights of 5-week-old pups (Table 8). Heart, lung, stomach, spleen, kidney, liver, uterus, ovaries, testes, and epididymis were weighed. All DNMT1 inhibitor treatment groups were similar with little difference from control. These results suggest that early embryonic treatment with the DNMT1 inhibitors Myb1, SAH, and RG108 does not affect postnatal development.

Table 8. Organ weights of 5 weeks embryo transferred mice

	Weight (g)			
	vehicle	**Myb1**	**SAH**	**RG108**
Body weight	19.927 ± 0.10	20.643 ± 0.65	19.716 ± 0.142	20.512 ± 1.00
Heart	0.195 ± 0.04	0.182 ± 0.05	0.14 ± 0.005	0.218 ± 0.20
Lungs	0.189 ± 0.01	0.191 ± 0.015	0.2 ± 0.005	0.14 ± 0.005
Stomach	0.185 ± 0.01	0.20 ± 0.008	0.25 ± 0.05	0.1584 ± 0.014
Spleen	0.113 ± 0.0.2	0.091 ± 0.002	0.086 ± 0.02	0.124 ± 0.01
Kidneys	0.257 ± 0.01	0.285 ± 0.013	0.283 ± 0.003	0.298 ± 0.02
Liver	0.997 ± 0.049	0.958 ± 0.010	0.72 ± 0.162	0.8712 ± 0.07
Testes	0.122 ± 0.017	0.15 ± 0.01	0.1 ± 0.02	0.1407 ± 0.02
Epididymis	0.029 ± 0.005	0.035 ± 0.005	0.029 ± 0.008	0.0307 ± 0.01
Uterus	0.037 ± 0.001	0.0305 ± 0.006	0.0285 ± 0.01	0.04 ± 0.01
ovaries	0.0045 ± 0.005	0.005 ± 0.001	0.0035 ± 0.001	0.004 ± 0.001

Mean ± S.D.

Comparison of mRNA profiling between DNMT1 modulators

Gene expression profiling in preimplantation embryo was studied with RNA-seq data mentioned at Materials and Methods. Considering the development rate, the 2-C stage, which is the first treatment point, the morula stage (84 h), which has high variation in phenotype between treatment groups and where compaction occurred, the hatching blastocyst (120 h), and the hatched blastocyst stage (144 h), which is the stage just before implantation, were selected. RNA seq was then performed. The transcriptomes of between treated group were shown no distinct clustering by PCA in 2-C stage and hatched blastocyst stage (Fig 10A). But at morula stage, SAH treated embryos were shown a higher variation. And at the hatching blastocyst stage, vehicle and Myb1, SAH and RG108 groups showed more similarity. It means that more dynamic transcriptomic change occurs in the morula and hatching blastocyst stage. A further GO analysis of the DEGs in embryo treated Myb1 revealed that the DEGs in carbohydrate metabolic, JAK-STAT signaling pathway, regulation of miRNA, intermediate filament genes were significantly enriched (Fig 10B). GO analysis of the DEGs in embryo treated SAH revealed that the DEGs in immune cell, intermediated filament cytoskeleton, peptidase regulation genes were significantly enriched (Fig 10C). The results of the GO analysis of RG108 and Myb14 were similar. GO analysis of the DEGs in embryo treated RG108 revealed that the DEGs in cell proliferation, carbohydrate metabolic, cytokine receptor activity related genes were significantly enriched (Fig 10D). Collectively the results suggest that the inactivity of DNMT1 implicates specific genetic pathways in fundamental biological function.

A

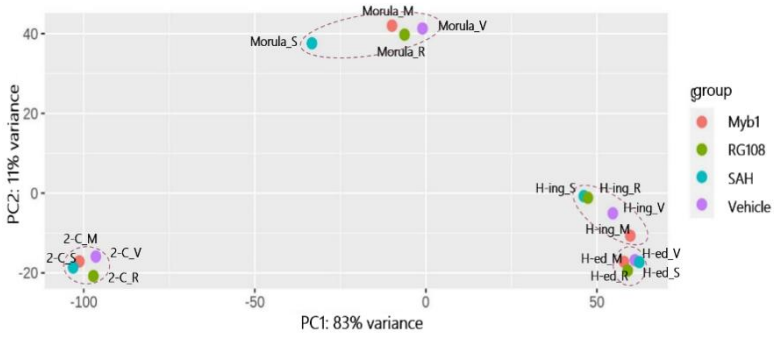
Morula_M
Morula_V
Morula_S
Morula_R
H-ing_S
H-ing_R
H-ing_V
H-ing_M
H-ed_M
H-ed_V
H-ed_R
H-ed_S
2-C_M
2-C_S
2-C_V
2-C_R
PC2: 11% variance
PC1: 83% variance
group
Myb1
RG108
SAH
Vehicle

B

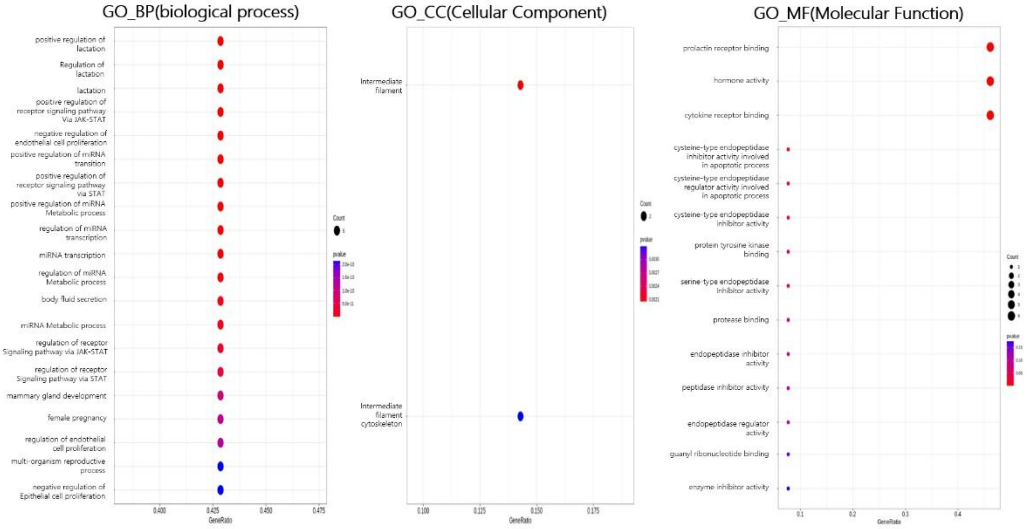
GO_BP(biological process)
GO_CC(Cellular Component)
GO_MF(Molecular Function)
positive regulation of lactation
Regulation of lactation
lactation
positive regulation of receptor signaling pathway Via JAK-STAT
negative regulation of endothelial cell proliferation
positive regulation of mRNA transition
positive regulation of receptor signaling pathway via STAT
positive regulation of mRNA Metabolic process
regulation of mRNA transcription
mRNA transcription
regulation of mRNA Metabolic process
body fluid secretion
mRNA Metabolic process
regulation of receptor Signaling pathway via JAK-STAT
regulation of receptor Signaling pathway via STAT
mammary gland development
female pregnancy
regulation of endothelial cell proliferation
multi-organism reproductive process
negative regulation of Epithelial cell proliferation
Intermediate filament
Intermediate filament cytoskeleton
prolactin receptor binding
hormone activity
cytokine receptor binding
cysteine-type endopeptidase inhibitor activity involved in apoptotic process
cysteine-type endopeptidase regulator activity involved in apoptotic process
cysteine-type endopeptidase inhibitor activity
protein tyrosine kinase binding
serine type endopeptidase inhibitor activity
protease binding
endopeptidase inhibitor activity
peptidase inhibitor activity
endopeptidase regulator activity
guanyl ribonucleotide binding
enzyme inhibitor activity
GeneRatio
Count
pvalue

C

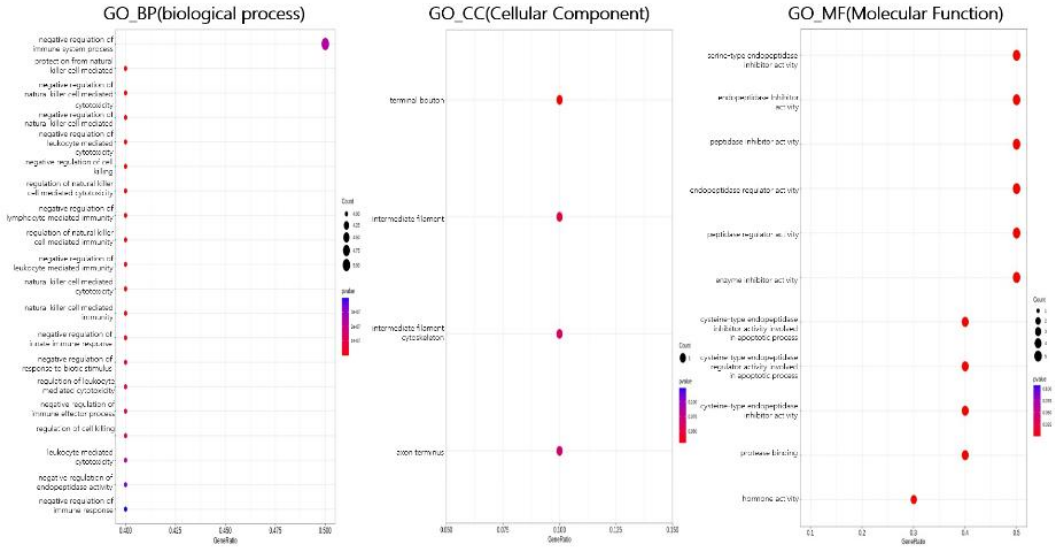
GO_BP(biological process)
GO_CC(Cellular Component)
GO_MF(Molecular Function)
terminal bouton
intermediate filament
intermediate filament cytoskeleton
axon terminus
serine-type endopeptidase inhibitor activity
endopeptidase inhibitor activity
peptidase inhibitor activity
endopeptidase regulator activity
peptidase regulator activity
enzyme inhibitor activity
cysteine-type endopeptidase inhibitor activity involved in apoptotic process
cysteine-type endopeptidase regulator activity involved in apoptotic process
cysteine-type endopeptidase inhibitor activity
protease binding
hormone activity

D

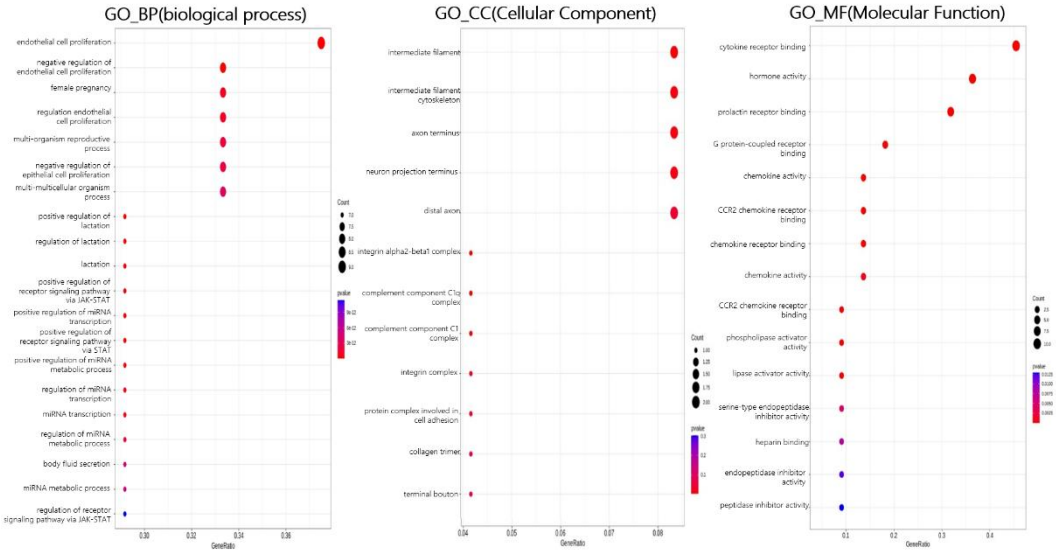
GO_BP(biological process)
GO_CC(Cellular Component)
GO_MF(Molecular Function)
endothelial cell proliferation
negative regulation of endothelial cell proliferation
female pregnancy
regulation endothelial cell proliferation
multi-organism reproductive process
negative regulation of epithelial cell proliferation
multi-multicellular organism process
positive regulation of lactation
regulation of lactation
lactation
positive regulation of receptor signaling pathway via JAK-STAT
positive regulation of miRNA transcription
positive regulation of receptor signaling pathway via STAT
positive regulation of miRNA metabolic process
regulation of miRNA transcription
miRNA transcription
regulation of miRNA metabolic process
body fluid secretion
miRNA metabolic process
regulation of receptor signaling pathway via JAK-STAT
intermediate filament
intermediate filament cytoskeleton
axon terminus
neuron projection terminus
distal axon
integrin alpha2-beta1 complex
complement component C1q complex
complement component C1 complex
integrin complex
protein complex involved in cell adhesion
collagen trimer
terminal bouton
cytokine receptor binding
hormone activity
prolactin receptor binding
G protein-coupled receptor binding
chemokine activity
CCR2 chemokine receptor binding
chemokine receptor binding
chemokine activity
CCR2 chemokine receptor binding
phospholipase activator activity
lipase activator activity
serine-type endopeptidase inhibitor activity
heparin binding
endopeptidase inhibitor activity
peptidase inhibitor activity

Figure 10. Global gene expression profiling on early stage mouse embryo through RNA sequencing

(A) The principle component plot shows the distribution of gene expression replicates for by treated group at 2-cell, Morula, Hatching blastocyst, Hatched blastocyst. (B-D) Representative GO term BP (biological process), CC (cellular component), MF (molecular function) enriched in embryo treated Myb1 (B) embryo treated SAH (C) embryo treated RG108 (D). *p* value indicates the significance of the enrichment.

DISCUSSION

DNA methylation is dramatically changed during early stage embryo development and DNMT1 inhibitors have positive or negative effects on embryo development (Yin et al. 2012; Zhang et al., 2015). the effects of three DNMT1 modulators on the expression of the *Prnp* during preimplantation embryonic stage were investigated using bank vole Prnp GPI KI mice. In WT early mice treated with 10 μM Myb1 resulted in increase the developmental rate to hatching blastocyst at 120 h, in KI mice embryo, it was similar to the vehicle. In 1 mM SAH-treated groups, the developmental rate decreased from 96 h (blastocyst) in WT and 72 h (8-cell) in KI, and in 20 μM RG108-treated embryos, the developmental rate was not different from vehicle in WT and significantly increased from 120 h (hatching blastocyst) in KI. The effects of the DNMT1 modulators were different by chemicals, the development to the hatching stage was increased by Myb1 and RG108, but not SAH.

To identify which genes are involved in the developmental rate effects of DNMT1 modulator treatment, the mRNA levels of the genes which are concerned with early embryonic potency and competency-related genes. In Myb1-treated embryos, *Cdx2*, a TE lineage related gene, was increased at 72 h (8-cell) in WT, and *Pou5f1*, a pluripotency related gene, continued to increase after the 84 h (morula) stage. The increase in these genes may have promoted blastocyst formation and increased the development rate. In KI, the expression of Pou5f1 was increased as in WT, but the developmental rate was not affected. In SAH-treated embryos, the expression of *Sox2*, a TE lineage-related gene, and *Dsc2*, a polarity-related gene, decreased in both WT and KI. In addition, *Pou5f1* was reduced in KI mice at 96 h (blastocyst) and 144 h (hatched blastocyst). The decrease was mainly in TE-related genes, and it is expected that this decrease

leads to a decrease in developmental rate. In RG108, *MuERV-L* was increased at 120 h (hatching blastocyst) in WT and *Cx32* was increased at 60 h (4-cell) in KI. The expression profiles were similar between chemicals except in Pou5f1 and Sox2 in background dependent manners.

The number of pups born from embryo transfer of DNMT1-treated embryos to surrogate mothers and the normal organization of the pups were examined, and the number of pups born from embryo transfer of Myb1-treated embryos was increased in WT and decreased in SAH, and there was no difference between the groups in the organ weights of the pups born. The expression of other genes should not be affected for normal development, and the imprinted genes and DNMT enzyme family genes were not affected. Those may be cause of normal development in the live pubs.

During oogenesis and preimplantation embryo development, DNA methylation plays critical roles in strictly regulating stimulation or repression of the development related genes and in timely establishing maternal and paternal imprints (Bartolomei and Ferguson-Smith, 2011). Following fertilization, maternal genome undergoes passive DNA demethylation throughout several round of DNA replication. The paternal genome undergoes active demethylation before DNA replication in zygote ensure (Messerschmidt et al., 2014). It is important that demethylation of parental genomes during zygotic genome activation (ZGA). At this time, we processed the DNMT1 modulator that helps with demethylation, and it showed elevated embryo development.

DNA methyltransferase inhibitors (DNMTi) are divided into nucleoside analogs and non-nucleoside analogs. The nucleoside analog and metabolizes DNMT before they are incorporated into DNA, so irreversible covalent degradation occurs and multiple side effects can occur. SAH is a non-nucleoside analog. On

the other hand, RG 108 is a non-nucleoside analog and this inhibits DNMT activity by Blocking the active site of DNMT enzyme, so Reversible inhibition of DNMT is possible and can exist stable. The DNMT1 inhibitor Myb1, which we want to study in this experiment, is also a non-nucleoside analog as a binding site specific small molecule. Myb1 was also designed through the process of CADD (Computer-Aided Drug Discovery) that basically relies on the computer modeling and predicting applications. Therefore, it can bind with DNMTs in a structurally stable manner through predicting Interatomic Bonds**.**

In addition, this study identified the expression pattern and location of PrP^c in mouse early embryo. Although it didn't affect the DNA methylation pattern, at 84 h (morula), mRNA was unchanged in WT and increased in both DNMT1 inhibitor-treated groups compared to vehicle in Protein. In KI, both mRNA and protein increased upon RG108 treatment. These results suggest that DNMT1 inhibitor may affect the expression of PrP^c via regulation of other region other than the CpG site of the promoter.

The epigenetic modulation might be involved in the chromatin remodeling, leading to a more permissive chromatin state and these changes could contribute to the proposed role of Myb1 in improving the efficiency of embryo development. The results show that treatment of early embryo with 10 μM Myb1 has no cytotoxic effect, results in significant increase in mRNA levels of *Pou5f1* and leads to improvement of developmental rate. Myb1 increase PrP^c levels at morula stage embryo without DNA methylation change.

On, summary, Myb1 increased Pou5f1 mRNA expression in WT mouse early embryos and improved the developmental potency. It did not affect the expression of imprinted genes and DNMT enzyme family genes and showed no

defect during embryonic development. It also altered PrP^c expression at the morula stage without changing the mRNA of *Prnp*.

In future experiment including, in vivo experiments and experiment targeting other regulating sites in the *Prnp* will help to know study the effect and role of *Prnp* on mouse early embryos.

REFERENCES

Alberio R, Campbell KH. Epigenetics and nuclear transfer. Lancet. 2003 Apr 12;361(9365):1239-40. doi: 10.1016/S0140-6736(03)13029-2. PMID: 12699948.

Andrews S, Krueger C, Mellado-Lopez M, Hemberger M, Dean W, Perez-Garcia V, Hanna CW. Mechanisms and function of de novo DNA methylation in placental development reveals an essential role for DNMT3B. Nat Commun. 2023 Jan 23;14(1):371. doi: 10.1038/s41467-023-36019-9. PMID: 36690623; PMCID: PMC9870994.

Assis RIF, Wiench M, Silvério KG, da Silva RA, Feltran GDS, Sallum EA, Casati MZ, Nociti FH Jr, Andia DC. RG108 increases NANOG and OCT4 in bone marrow-derived mesenchymal cells through global changes in DNA modifications and epigenetic activation. PLoS One. 2018 Dec 3;13(12):e0207873. doi: 10.1371/journal.pone.0207873. PMID: 30507955; PMCID: PMC6277091.

Azevedo Portilho N, Saini D, Hossain I, Sirois J, Moraes C, Pastor WA. The DNMT1 inhibitor GSK-3484862 mediates global demethylation in murine embryonic stem cells. Epigenetics Chromatin. 2021 Dec 15;14(1):56. doi: 10.1186/s13072-021-00429-0. PMID: 34906184; PMCID: PMC8672470.

Bartolomei MS, Ferguson-Smith AC. Mammalian genomic imprinting. Cold Spring Harb Perspect Biol. 2011 Jul 1;3(7):a002592. doi: 10.1101/cshperspect.a002592. PMID: 21576252; PMCID: PMC3119911.

Caughey B, Baron GS, Chesebro B, Jeffrey M. Getting a grip on prions: oligomers, amyloids, and pathological membrane interactions. Annu Rev Biochem. 2009;78:177-204. doi: 10.1146/annurev.biochem.78.082907.145410. PMID: 19231987; PMCID: PMC2794486.

Cohen FE, Pan KM, Huang Z, Baldwin M, Fletterick RJ, Prusiner SB. Structural clues to prion replication. Science. 1994 Apr 22;264(5158):530-1. doi: 10.1126/science.7909169. PMID: 7909169.

Dalai W, Matsuo E, Takeyama N, Kawano J, Saeki K. CpG site DNA methylation patterns reveal a novel regulatory element in the mouse prion protein gene. J Vet Med Sci. 2017 Jan 20;79(1):100-107. doi: 10.1292/jvms.16-0390. Epub 2016 Sep 26. PMID: 27666463; PMCID: PMC5289245.

Gao R, Wang C, Gao Y, Xiu W, Chen J, Kou X, Zhao Y, Liao Y, Bai D, Qiao Z, Yang L, Wang M, Zang R, Liu X, Jia Y, Li Y, Zhang Y, Yin J, Wang H, Wan X, Liu W, Zhang Y, Gao S. Inhibition of Aberrant DNA Re-methylation Improves Post-implantation Development of Somatic Cell Nuclear Transfer Embryos. Cell Stem Cell. 2018 Sep 6;23(3):426-435.e5. doi: 10.1016/j.stem.2018.07.017. Epub 2018 Aug 23. PMID: 30146410.

Giraldo AM, DeCourcy K, Ball SF, Hylan D, Ayares DL. Gene expression of Dnmt1 isoforms in porcine oocytes, embryos, and somatic cells. Cell Reprogram. 2013 Aug;15(4):309-21. doi: 10.1089/cell.2012.0088. Epub 2013 Jun 28. PMID: 23808878; PMCID: PMC3725799.

Go G, Lee SH. The Cellular Prion Protein: A Promising Therapeutic Target for Cancer. Int J Mol Sci. 2020 Dec 2;21(23):9208. doi: 10.3390/ijms21239208. PMID: 33276687; PMCID: PMC7730109.

Haggerty C, Kretzmer H, Riemenschneider C, Kumar AS, Mattei AL, Bailly N, Gottfreund J, Giesselmann P, Weigert R, Brändl B, Giehr P, Buschow R, Galonska C, von Meyenn F, Pappalardi MB, McCabe MT, Wittler L, Giesecke-Thiel C, Mielke T, Meierhofer D, Timmermann B, Müller FJ, Walter J, Meissner A. Dnmt1 has de novo activity targeted to transposable elements. Nat Struct Mol Biol. 2021 Jul;28(7):594-603. doi: 10.1038/s41594-021-00603-8. Epub 2021 Jun 17. PMID: 34140676; PMCID: PMC8279952.

Hirasawa R, Chiba H, Kaneda M, Tajima S, Li E, Jaenisch R, Sasaki H. Maternal and zygotic Dnmt1 are necessary and sufficient for the maintenance of DNA methylation imprints during preimplantation development. Genes Dev. 2008 Jun 15;22(12):1607-16. doi: 10.1101/gad.1667008. PMID: 18559477; PMCID: PMC2428059.

Ito T, Kubiura-Ichimaru M, Murakami Y, Bogutz AB, Lefebvre L, Suetake I, Tajima S, Tada M. DNMT1 regulates the timing of DNA methylation by DNMT3 in an enzymatic activity-dependent manner in mouse embryonic stem cells. PLoS One. 2022 Jan 5;17(1):e0262277. doi: 10.1371/journal.pone.0262277. PMID: 34986190; PMCID: PMC8730390.

Jeltsch A, Ehrenhofer-Murray A, Jurkowski TP, Lyko F, Reuter G, Ankri S, Nellen W, Schaefer M, Helm M. Mechanism and biological role of Dnmt2 in Nucleic Acid Methylation. RNA Biol. 2017 Sep 2;14(9):1108-1123. doi: 10.1080/15476286.2016.1191737. Epub 2016 May 27. PMID: 27232191; PMCID: PMC5699548.

Jeon BG, Coppola G, Perrault SD, Rho GJ, Betts DH, King WA. S-adenosylhomocysteine treatment of adult female fibroblasts alters X-chromosome inactivation and improves in vitro embryo development after somatic cell nuclear transfer. Reproduction. 2008 Jun;135(6):815-28. doi: 10.1530/REP-07-0442. Epub 2008 Feb 27. PMID: 18304987.

Kim DH, Ren C, Ryou C, Li J. Direct interaction of DNMT inhibitors to PrP^C suppresses pathogenic process of prion. Acta Pharm Sin B. 2019 Sep;9(5):952-959. doi: 10.1016/j.apsb.2019.04.001. Epub 2019 Apr 18. PMID: 31649845; PMCID: PMC6804459.

Ko YG, Nishino K, Hattori N, Arai Y, Tanaka S, Shiota K. Stage-by-stage change in DNA methylation status of Dnmt1 locus during mouse early development. J Biol Chem. 2005 Mar 11;280(10):9627-34. doi: 10.1074/jbc.M413822200. Epub 2005 Jan 4. PMID: 15634679.

Kondo N, Tohnai G, Sahashi K, Iida M, Kataoka M, Nakatsuji H, Tsutsumi Y, Hashizume A, Adachi H, Koike H, Shinjo K, Kondo Y, Sobue G, Katsuno M. DNA methylation inhibitor attenuates polyglutamine-induced neurodegeneration by regulating Hes5. EMBO Mol Med. 2019 May;11(5):e8547. doi: 10.15252/emmm.201708547. PMID: 30940675; PMCID: PMC6505579.

Lee JH, Yun CW, Han YS, Kim S, Jeong D, Kwon HY, Kim H, Baek MJ, Lee SH. Melatonin and 5-fluorouracil co-suppress colon cancer stem cells by regulating cellular prion protein-Oct4 axis. J Pineal Res. 2018 Nov;65(4):e12519. doi: 10.1111/jpi.12519. Epub 2018 Aug 24. Erratum in: J Pineal Res. 2020 May;68(4):e12650. doi: 10.1111/jpi.12650. PMID: 30091203.

Lyko F, Brown R. DNA methyltransferase inhibitors and the development of epigenetic cancer therapies. J Natl Cancer Inst. 2005 Oct 19;97(20):1498-506. doi: 10.1093/jnci/dji311. PMID: 16234563.

Manson JC, Clarke AR, Hooper ML, Aitchison L, McConnell I, Hope J. 129/Ola mice carrying a null mutation in PrP that abolishes mRNA production are developmentally normal. Mol Neurobiol. 1994 Apr-Jun;8(2-3):121-7. doi: 10.1007/BF02780662. PMID: 7999308.

Messerschmidt DM, Knowles BB, Solter D. DNA methylation dynamics during epigenetic reprogramming in the germline and preimplantation embryos. Genes Dev. 2014 Apr 15;28(8):812-28. doi: 10.1101/gad.234294.113. PMID: 24736841; PMCID: PMC4003274.

Miranda A, Pericuesta E, Ramírez MÁ, Gutierrez-Adan A. Prion protein expression regulates embryonic stem cell pluripotency and differentiation. PLoS One. 2011 Apr 4;6(4):e18422. doi: 10.1371/journal.pone.0018422. PMID: 21483752; PMCID: PMC3070729.

Monk D. Germline-derived DNA methylation and early embryo epigenetic reprogramming: The selected survival of imprints. Int J Biochem Cell Biol. 2015 Oct;67:128-38. doi: 10.1016/j.biocel.2015.04.014. Epub 2015 May 9. PMID: 25966912.

O'Doherty AM, O'Shea LC, Fair T. Bovine DNA methylation imprints are established in an oocyte size-specific manner, which are coordinated with the expression of the DNMT3 family proteins. Biol Reprod. 2012 Mar 19;86(3):67. doi: 10.1095/biolreprod.111.094946. PMID: 22088914.

Petrussa L, Van de Velde H, De Rycke M. Dynamic regulation of DNA methyltransferases in human oocytes and preimplantation embryos after assisted reproductive technologies. Mol Hum Reprod. 2014 Sep;20(9):861-74. doi: 10.1093/molehr/gau049. Epub 2014 Jul 3. PMID: 24994815.

Prusiner SB. Prions. Proc Natl Acad Sci U S A. 1998 Nov 10;95(23):13363-83. doi: 10.1073/pnas.95.23.13363. PMID: 9811807; PMCID: PMC33918.

Sigurdson CJ, Bartz JC, Glatzel M. Cellular and Molecular Mechanisms of Prion Disease. Annu Rev Pathol. 2019 Jan 24;14:497-516. doi: 10.1146/annurev-pathmechdis-012418-013109. Epub 2018 Oct 24. PMID: 30355150; PMCID: PMC9071098.

Song X, Liu Z, He H, Wang J, Li H, Li J, Li F, Jiang Z, Huan Y. Dnmt1s in donor cells is a barrier to SCNT-mediated DNA methylation reprogramming in pigs. Oncotarget. 2017 May 23;8(21):34980-34991. doi: 10.18632/oncotarget.16507. PMID: 28380421; PMCID: PMC5471028.

Sun HL, Meng LN, Zhao X, Jiang JR, Liu QY, Shi DS, Lu FH. Effects of DNA methyltransferase inhibitor RG108 on methylation in buffalo adult fibroblasts and subsequent embryonic development following somatic cell nuclear transfer. Genet Mol Res. 2016 Sep 2;15(3). doi: 10.4238/gmr.15038455. PMID: 27706684.

Turek-Plewa J, Jagodziński PP. The role of mammalian DNA methyltransferases in the regulation of gene expression. Cell Mol Biol Lett. 2005;10(4):631-47. PMID: 16341272.

Uysal F, Akkoyunlu G, Ozturk S. Dynamic expression of DNA methyltransferases (DNMTs) in oocytes and early embryos. Biochimie. 2015 Sep;116:103-13. doi: 10.1016/j.biochi.2015.06.019. Epub 2015 Jul 2. PMID: 26143007.

Uysal F, Cinar O, Can A. Knockdown of Dnmt1 and Dnmt3a gene expression disrupts preimplantation embryo development through global DNA methylation. J Assist Reprod Genet. 2021 Dec;38(12):3135-3144. doi: 10.1007/s10815-021-02316-9. Epub 2021 Sep 17. PMID: 34533678; PMCID: PMC8666391.

Uysal F, Ozturk S, Akkoyunlu G. DNMT1, DNMT3A and DNMT3B proteins are differently expressed in mouse oocytes and early embryos. J Mol Histol. 2017 Dec;48(5-6):417-426. doi: 10.1007/s10735-017-9739-y. Epub 2017 Oct 13. PMID: 29027601.

Wei Y, Huan Y, Shi Y, Liu Z, Bou G, Luo Y, Zhang L, Yang C, Kong Q, Tian J, Xia P, Sun QY, Liu Z. Unfaithful maintenance of methylation imprints due to loss of maternal nuclear Dnmt1 during somatic cell nuclear transfer. PLoS One. 2011;6(5):e20154. doi: 10.1371/journal.pone.0020154. Epub 2011 May 20. PMID: 21625467; PMCID: PMC3098883.

Yin LJ, Zhang Y, Lv PP, He WH, Wu YT, Liu AX, Ding GL, Dong MY, Qu F, Xu CM, Zhu XM, Huang HF. Insufficient maintenance DNA methylation is associated with abnormal embryonic development. BMC Med. 2012 Mar 13;10:26. doi: 10.1186/1741-7015-10-26. PMID: 22413869; PMCID: PMC3355050.

Zhai Y, Zhang Z, Yu H, Su L, Yao G, Ma X, Li Q, An X, Zhang S, Li Z. Dynamic Methylation Changes of DNA and H3K4 by RG108 Improve Epigenetic Reprogramming of Somatic Cell Nuclear Transfer Embryos in Pigs. Cell Physiol Biochem. 2018;50(4):1376-1397. doi: 10.1159/000494598. Epub 2018 Oct 24. PMID: 30355946.

Zhang S, Chen X, Wang F, An X, Tang B, Zhang X, Sun L, Li Z. Aberrant DNA methylation reprogramming in bovine SCNT preimplantation embryos. Sci Rep. 2016 Jul 26;6:30345. doi: 10.1038/srep30345. PMID: 27456302; PMCID: PMC4960566.

Zhang S, Tang B, Fan C, Shi L, Zhang X, Sun L, Li Z. Effect of DNMT inhibitor on bovine parthenogenetic embryo development. Biochem Biophys Res Commun. 2015 Oct 23;466(3):505-11. doi: 10.1016/j.bbrc.2015.09.060. Epub 2015 Sep 14. PMID: 26381173.

논문개요

Prnp 유전자의 산물은 발달과 질병에 관여하는 기능성 분자이다. 프리온 질환의 원인 중 하나는 조직 내 PrPC 의 양때문이며, 프리온으로부터 보호하는 방법으로 PrPC 의 발현 수준을 조절하는 것이 제안되고 있다. 또한 PrPC 는 여러 신호 전달 경로를 통해 세포 증식, 전이, 약물 내성, 암 줄기세포 표현형 등에 영향을 미칠 수 있다. DNA 메틸화는 주요 후성유전학적 메커니즘이며 레트로 트랜스포존의 침묵, 게놈 각인 및 세포 분화에 중요한 역할을 한다. 후성유전학적 변형은 초기 배아 단계에서 일어나지만, 난할 과정에서의 후성유전학적 조절은 완전히 밝혀지지 않았다. 이 연구에서는 난할 시기에서 Prnp 의 발현을 조사하고 DNMT1 조절제인 Myb1, SAH, RG108 을 통해 배아 발달 관련 유전자의 변화를 야생형 생쥐와 뱅크볼 Prnp 동형접합 생쥐에서 평가했다. 야생형 생쥐에서 배반포기 단계로의 발달은 10μM My 에서 대조군보다 유의하게 높았지만 1mM SAH 에서는 그렇지 않았다. *MuERV-L, Cdx2, Sox2, Cx32, Dsc2, Yap, Cdh1, Pou5f1, Nanog* 와 같은 분화능 관련 유전자 및 계통 관련 유전자의 발현도 억제제 특이적 패턴에 따라 변형되었다. SAH 를 처리한 그룹은 발달 속도 감소와 마찬가지로 위 유전자들에서 특히 비정상적인 발현을 보였다. 한편, Myb1 을 처리한 8 세포기 배아에서는 *Cdx2* 발현이 증가했고, 상실배 단계 이후에는 *Pou5f1* 유전자 수준도 다른 그룹에 비해 유의하게 증가했다. KI 생쥐에서도 마찬가지로 SAH 를 처리한 배아에서 위 유전자들의 발현 감소가 나타났고 Myb1 을 처리했을 때 부화진행 포배 단계에서 *Pou5f1* 유전자 수준이 유의적으로 증가했다. 각인유전자와 DNMT 유전자들의 발현도 분석해보았을 때 야생형과 뱅크볼 *Prnp* 동형접합 생쥐에서 유의적인 변화를 보이지 않았다. 그리고 DNMT1 억제제가 PRNP 발현에 영향을 미치는지 조사하기 위해 마우스 초기 배아에서 *Prnp* 와 PrP 의 발현 프로파일을 확인했다. 야생형에서 mRNA 발현은 유의적인 변화를 보이지 않았지만 상실배 단계에서 PrP 단백질은 대조군에 비해서 유의적으로 증가했다. 뱅크볼 *Prnp* 동형접합 생쥐에서는 RG108 을 처리한 상실배 단계의 배아가 mRNA 와 단백질에서 모두 유의적으로 증가했다. 위 DNMT1 억제제들이 *Prnp* 유전자의 CpG 영역의

메틸화를 조절하여 발현을 조절하는 지를 조사하기 위해 아황산수소 염기서열분석을 진행했지만 이 영역을 통하여 *Prnp* 발현이 조절되는 것은 아님을 밝혔다. 이후, DNMT1 억제제를 처리하여 키운 배아를 대리모에 배 이식을 함으로서 배아 발달과 성장에 영향을 어떤 영향을 미치는 지를 조사했다. Myb1 을 처리해서 배아의 배 이식 후 새끼가 태어날 확률이 대조군에 비해 유의적으로 증가했고 SAH 처리한 배아에서는 유의적으로 감소했다. 배 이식 후 태어난 뒤 5 주령된 새끼의 장기 무게를 비교했고 모든 그룹간 유의적인 차이는 없었다. RNA 시퀀스 분석 결과 Myb1 처리 배아에서 탄수화물 대사 관련 유전자, SAH 에서 면역 관련 유전자, RG108 에서 세포 증식 관련 유전자의 발현이 높은 것으로 나타났다. 이를 종합해 볼 때, DNMT1 억제제에 특이적으로 발생 관련 유전자 발현이 조절되며, Myb1 이 초기 배아 발달에 유용한 DNMT1 억제제로서 Prnp 발현 조절과 함께 초기 배아 발달에 유용한 것으로 추정된다.